Relative Abundances of Stable Isotopes [%]

Z		1	2	3	4	5	6	7	8	9	10	11	12	13	14	15	16	17	18	19	20	21	22	23	24	25	26	27	28	29	30	31	
1	H	100	.015																														H
2	He			.000	100																												He
3	Li						7.5	92.5																									Li
4	Be									100																							Be
5	B										20	80																					B
6	C												98.9	1.11																			C
7	N														99.6	.360																	N
8	O																99.8	.040	.200														O
9	F																			100													F
10	Ne																				90.5	.270	9.22										Ne
11	Na																							100									Na
12	Mg																								79	10	11						Mg
13	Al																											100					Al
14	Si																												92.2	4.67	3.1		Si
15	P																															100	P

Z		32	33	34	35	36	37	38	39	40	41	42	43	44	45	46	47	48	49	50	51	52	53	54	55	56	57	58					
16	S	95	.760	4.22		.020																											S
17	Cl				75.8		24.2																										Cl
18	Ar					.340		.070		99.6																							Ar
19	K								93.3	.010	6.73																						K
20	Ca									96.9		.647	.135	2.09		.004		.187															Ca
21	Sc														100																		Sc
22	Ti															8	7.5	73.7	5.5	5.3													Ti
23	V																			.250	99.8												V
24	Cr																			4.35		83.8	9.5	2.36									Cr
25	Mn																								100								Mn
26	Fe																							5.8		91.8	2.1	.300					Fe

Z		58	59	60	61	62	63	64	65	66	67	68	69	70	71	72	73	74	75	76	77	78	79	80	81	82							
26	Fe *	.300																															Fe *
27	Co		100																														Co
28	Ni	68.3		26.1	1.13	3.59		.910																									Ni
29	Cu						69.2		30.8																								Cu
30	Zn							48.6		27.9	4.1	18.8		.600																			Zn
31	Ga												60		40																		Ga
32	Ge													20.5		27.4	7.8	36.5		7.8													Ge
33	As																		100														As
34	Se																	.900		9	7.6	23.5		49.8		9.2							Se

Z		78	79	80	81	82	83	84	85	86	87	88	89	90	91	92	93	94	95	96	97	98	99	100	101	102	103	104					
34	Se *	23.5		49.8		9.2																											Se *
35	Br		50.7		49.3																												Br
36	Kr	.350		2.25		11.6	11.5	56.9		17.4																							Kr
37	Rb								72.2		27.8																						Rb
38	Sr							.500		9.9	7	82.6																					Sr
39	Y												100																				Y
40	Zr													51.4	11.2	17.1		17.5		2.8													Zr
41	Nb																100																Nb
42	Mo															14.8		9.3	15.9	16.7	9.6	24.1		9.6									Mo
44	Ru																			5.5		1.9	12.7	12.6	17.1	31.6		18.6					Ru
45	Rh																										100						Rh

Z		102	103	104	105	106	107	108	109	110	111	112	113	114	115	116	117	118	119	120	121	122	123	124	125	126	127	128	129	130			
44	Ru *	31.6		18.6																													Ru *
45	Rh		100																														Rh
46	Pd	1		11	22.2	27.3		26.7		11.8																							Pd
47	Ag						51.8		48.2																								Ag
48	Cd					1.2		.900		12.4	12.8	24	12.3	28.8		7.6																	Cd
49	In												4.3		95.7																		In
50	Sn											1		.700	.400	14.7	7.7	24.3	8.6	32.4		4.6		5.6									Sn
51	Sb																				57.3		42.7										Sb
52	Te																			.100		2.5	.900	4.6	7	18.7		31.7		34.5			Te
53	I																										100						I

Z		124	125	126	127	128	129	130	131	132	133	134	135	136	137	138	139	140	141	142	143	144	145	146	147	148	149	150	151	152	153	154	
50	Sn *	5.6																															Sn *
52	Te *	4.6	7	18.7		31.7		34.5																									Te *
53	I				100																												I
54	Xe	.100		.100		1.9	26.4	4.1	21.2	26.9		10.4		8.9																			Xe
55	Cs										100																						Cs
56	Ba							.100		.100		2.4	6.6	7.9	11.2	71.7																	Ba
57	La															.090	99.9																La
58	Ce													.200		.300		88.4		11.1													Ce
59	Pr																		100														Pr
60	Nd																			27.2	12.2	23.8	8.3	17.2		5.7		5.6					Nd
62	Sm																					3.1			15.1	11.3	13.9	7.4		26.6		22.6	Sm
63	Eu																												47.8		52.2		Eu

Z		152	153	154	155	156	157	158	159	160	161	162	163	164	165	166	167	168	169	170	171	172	173	174	175	176	177	178	179	180			
62	Sm *	26.6		22.6																													Sm *
63	Eu *		52.2																														Eu *
64	Gd	.200		2.2	14.8	20.5	15.7	24.8		21.8																							Gd
65	Tb								100																								Tb
66	Dy					.060		.100		2.34	18.9	25.5	24.9	28.2																			Dy
67	Ho														100																		Ho
68	Er											.100		1.6		33.4	22.9	27		15													Er
69	Tm																		100														Tm
70	Yb																	.100		3.1	14.3	21.9	16.2	31.7		12.7							Yb
71	Lu																								97.4	2.6							Lu
72	Hf																							.200		5.2	18.5	27.1	13.8	35.2			Hf

Z		180	181	182	183	184	185	186	187	188	189	190	191	192	193	194	195	196	197	198	199	200	201	202	203	204	205	206	207	208	209		
72	Hf *	35.2																															Hf *
73	Ta	.012	100																														Ta
74	W	.100		26.3	14.3	30.7		28.6																									W
75	Re						37.4		62.6																								Re
76	Os					.020		1.58	1.6	13.3	16.1	26.4		41																			Os
77	Ir												37.3		62.7																		Ir
78	Pt											.010		.790		32.9	33.8	25.3		7.2													Pt
79	Au																		100														Au
80	Hg																	.200		10.1	16.9	23.1	13.2	29.7		6.8							Hg
81	Tl																								29.5		70.5						Tl
82	Pb																									1.4		24.1	22.1	52.4			Pb
83	Bi																														100		Bi

* = incomplete (not all isotopes are shown in the same line)

FJ Stadermann 07/2010

Ion sources: EI

- EI is most common for GC detection
  - Electron ionization (NOT electron impact ionization)
- Many events possible in an electron-neutral collision
  - *excitation*

$$e^- + \text{A-B-C} = \text{A-B-C}^* \text{ (not detected)}$$

  - *electron capture*

$$e^- + \text{A-B-C} = \text{A-B-C}^- \text{ (not detected in positive mode)}$$

  - *Ionization*

$$e^- + \text{A-B-C} = \text{A-B-C}^{+\cdot} + 2e^-$$

  - *ionization w/ excitation (w/ or w/out rearrangement)*

$$e^- + \text{A-B-C} \rightarrow \text{A-B-C}^{+\cdot *} + 2e^- \rightarrow \text{A} + \left(\text{B-C}\right)^{+\cdot}$$
$$\rightarrow \text{A}^{\cdot} + \left(\text{B-C}\right)^{+}$$
$$\rightarrow \text{A}^{+\cdot} + \left(\text{B-C}\right)$$
$$\rightarrow \left(\text{A-C}\right)^{+\cdot} + \text{B etc.}$$

  - multiple ionization (/ or w/out excitation, dissociation, rearrangement etc.)

$$e^- + \text{A-B-C} = \text{A-B-C}^{2+\cdot} + 3e^-$$

Ion sources: EI

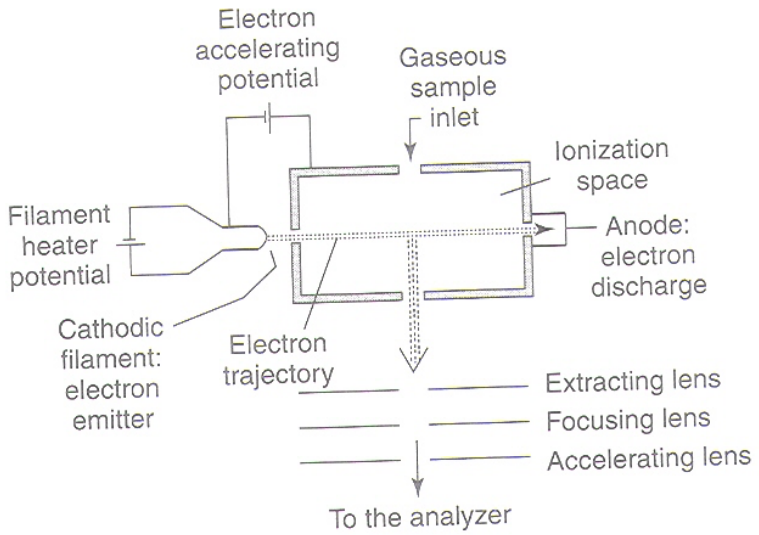

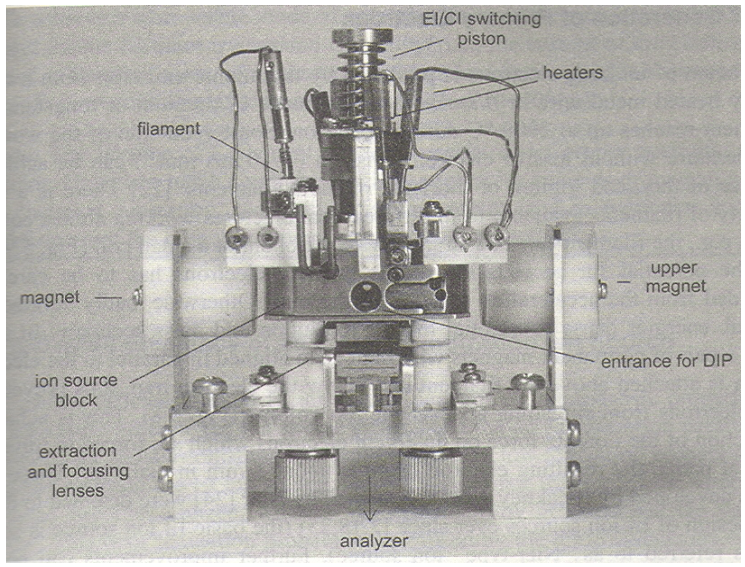

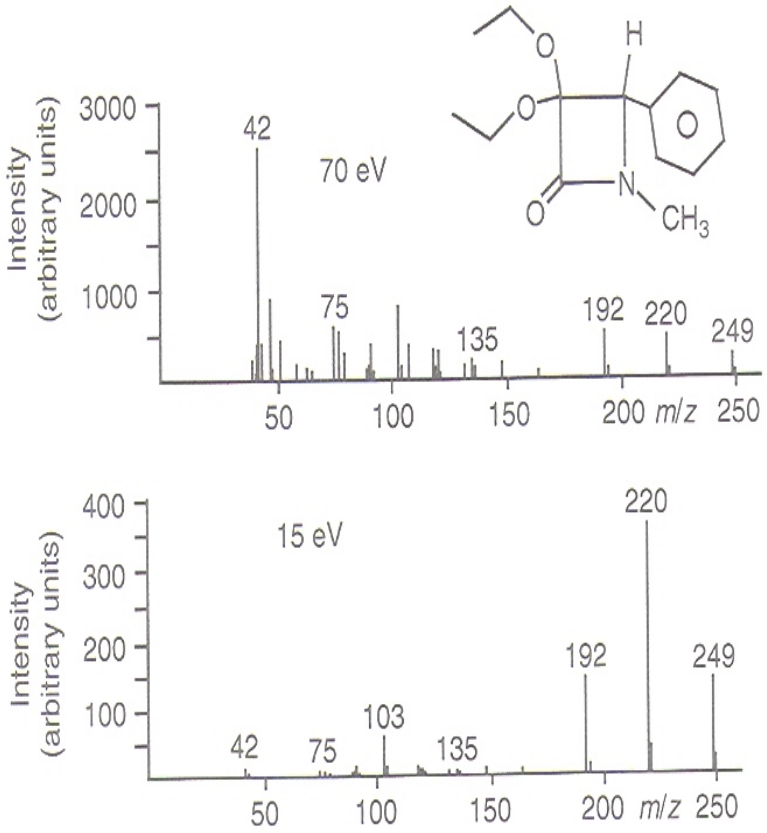

EI spectra of beta lactam at different e^- energies

de Hoffmann, E.; Stroobant, V. *Mass Spectrometry: Principles and Applications,* 2nd Ed; Wiley: New York, 2004.

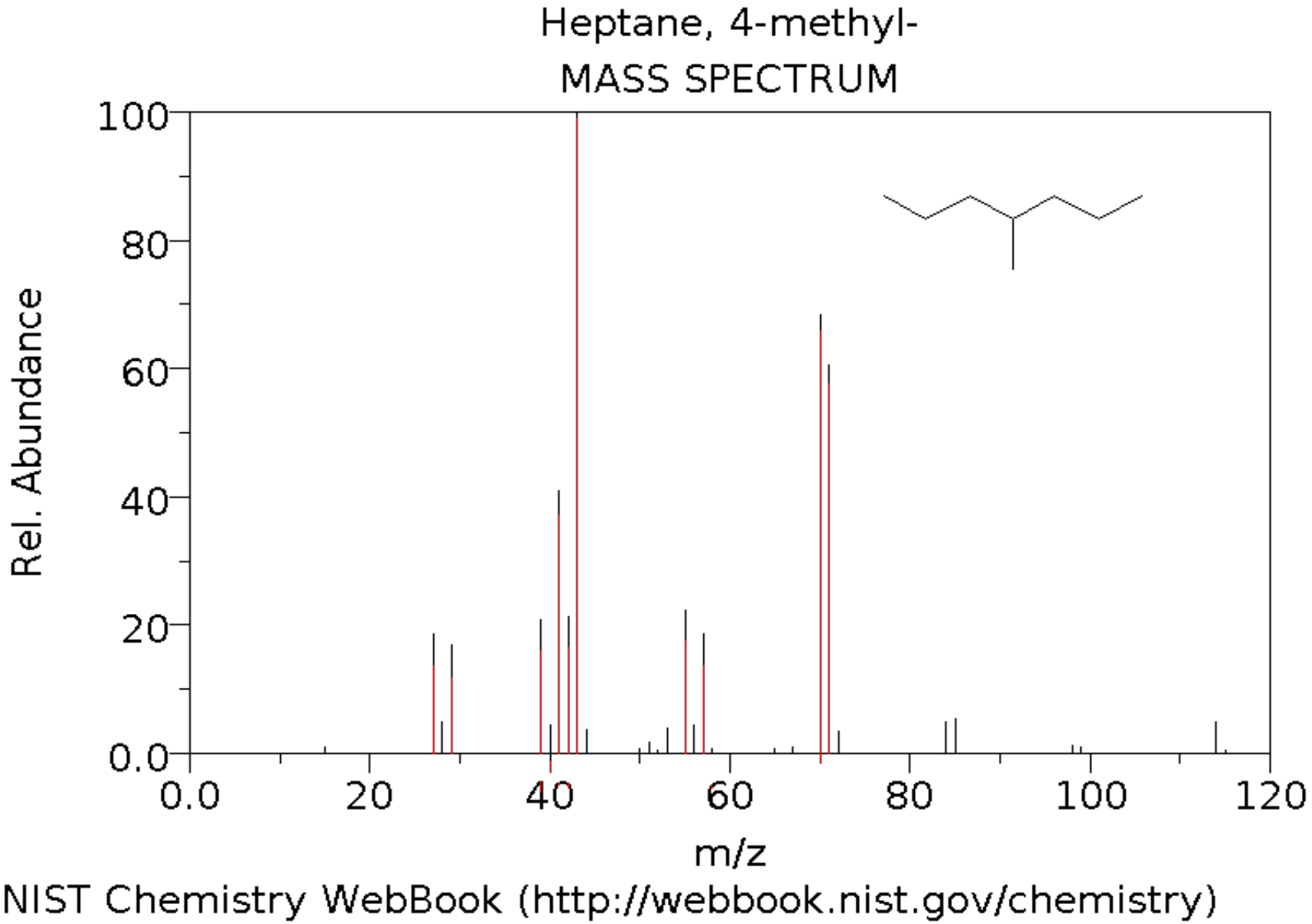

NIST Chemistry WebBook (http://webbook.nist.gov/chemistry)

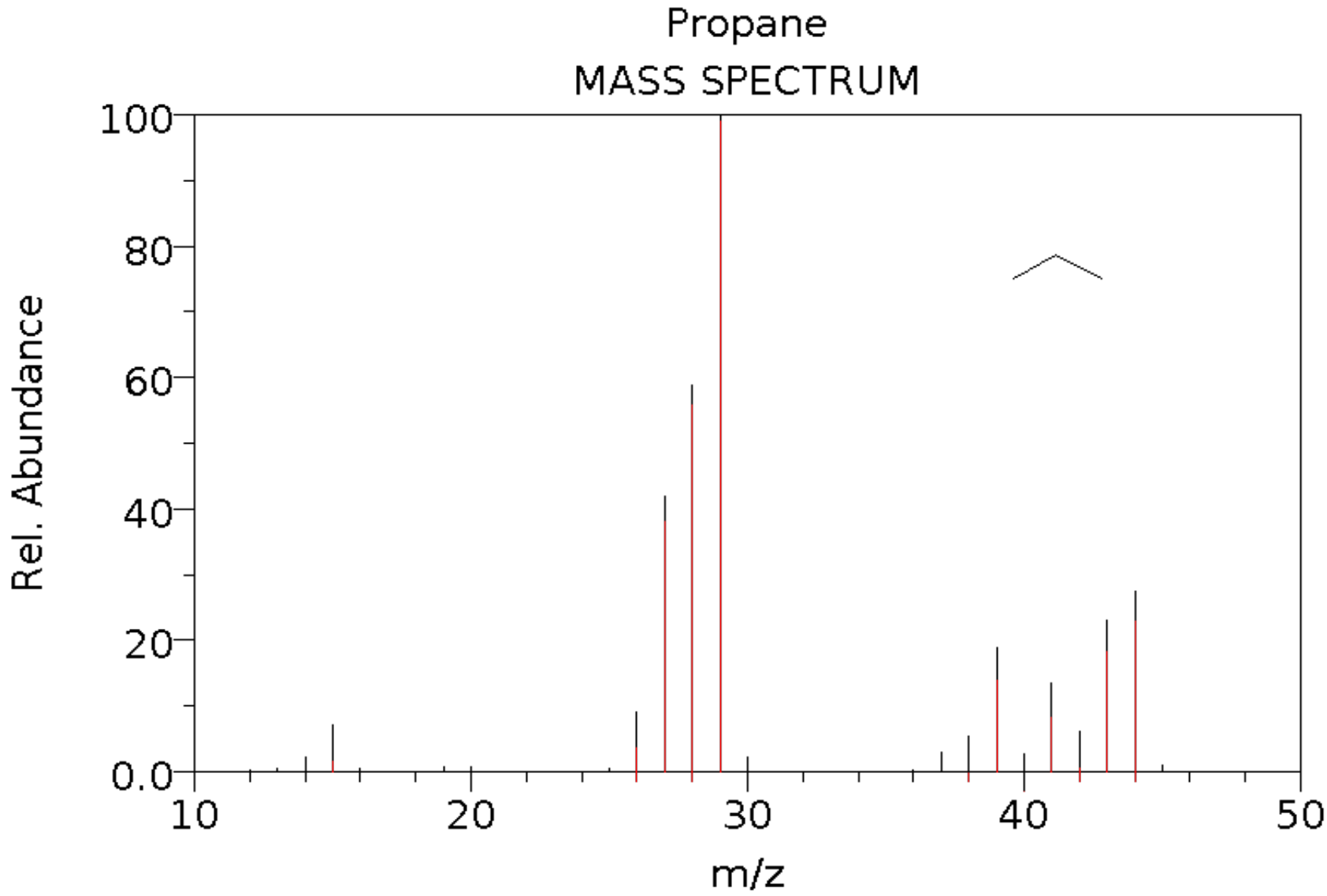

NIST Chemistry WebBook (http://webbook.nist.gov/chemistry)

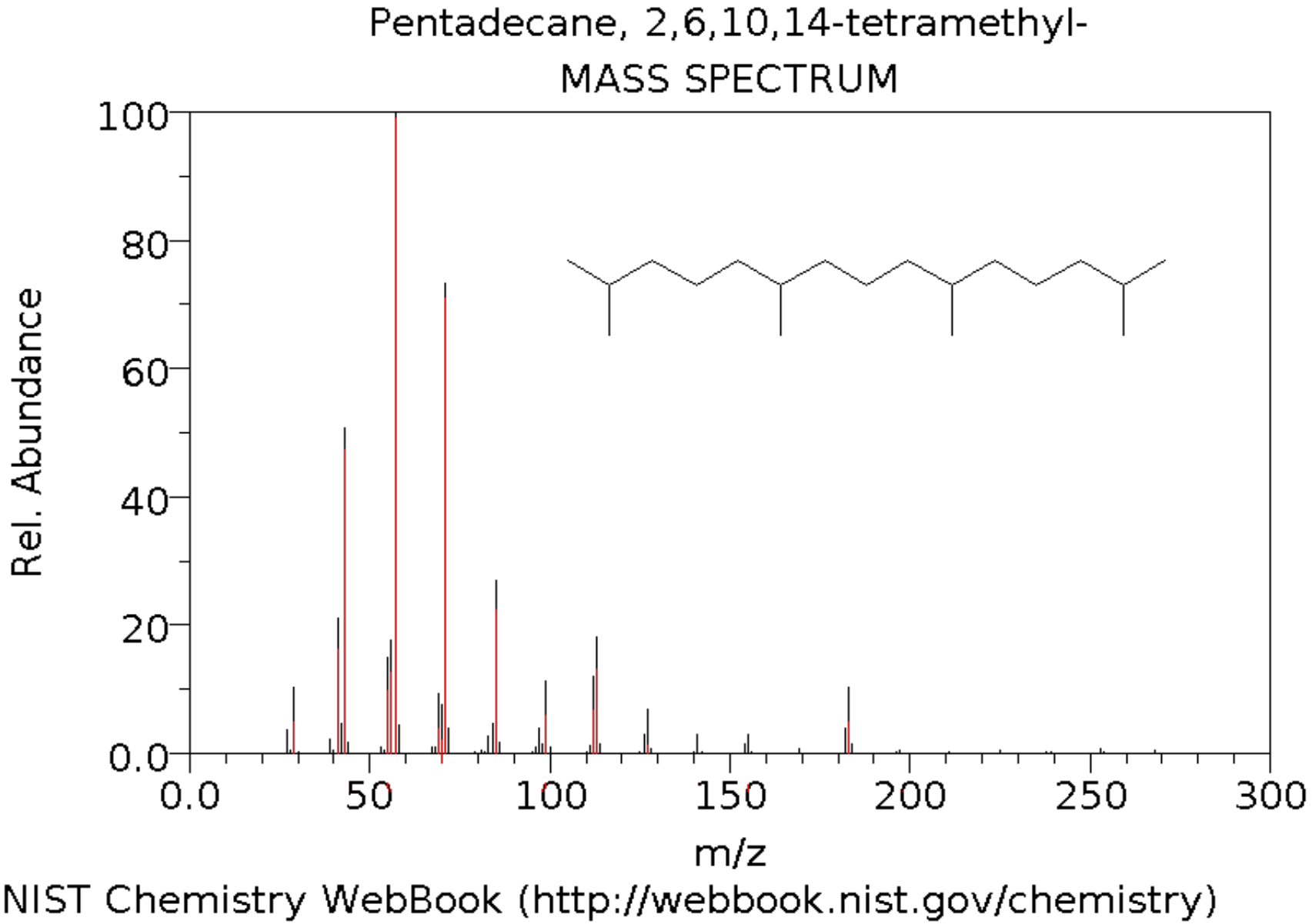

NIST Chemistry WebBook (http://webbook.nist.gov/chemistry)

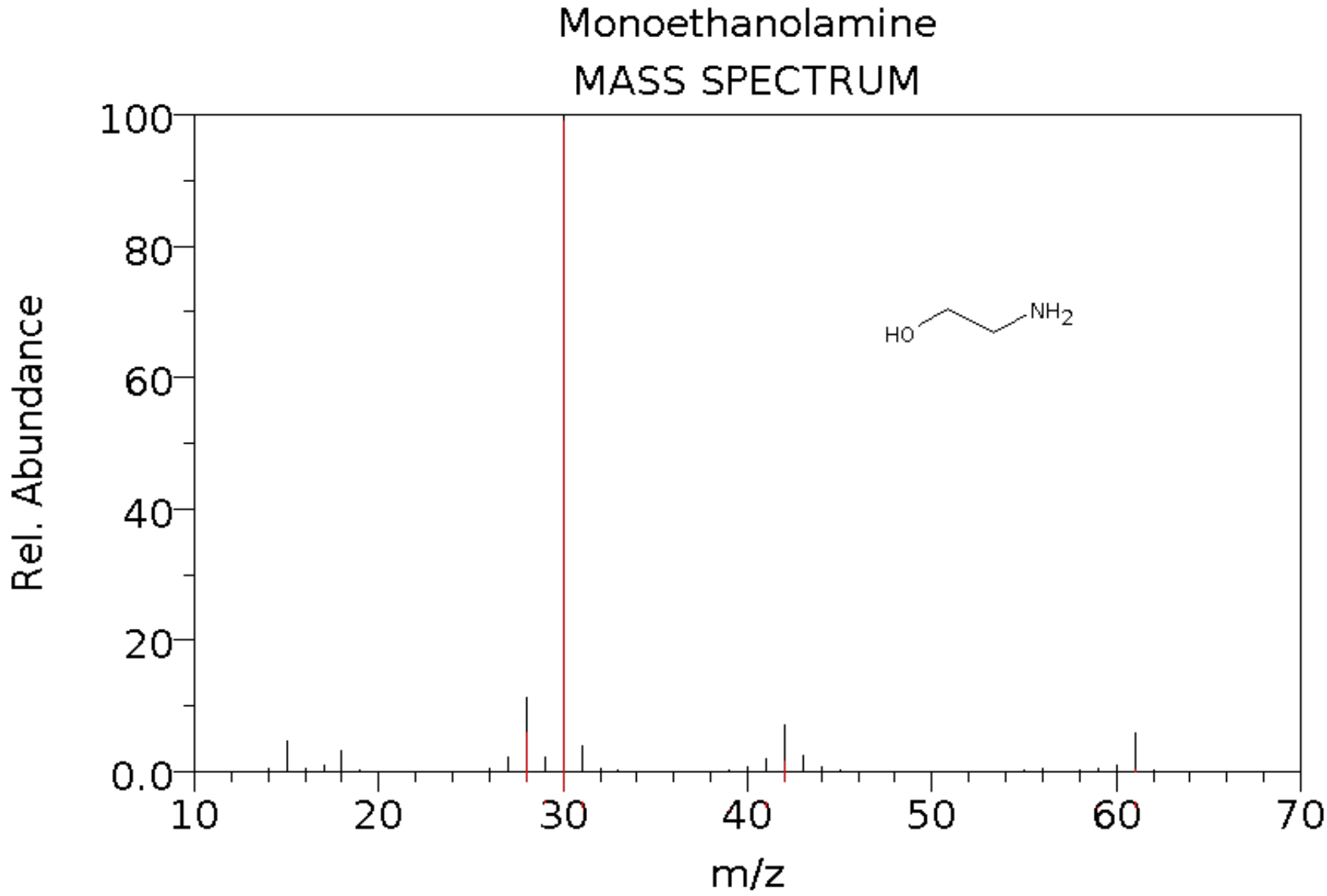

NIST Chemistry WebBook (http://webbook.nist.gov/chemistry)

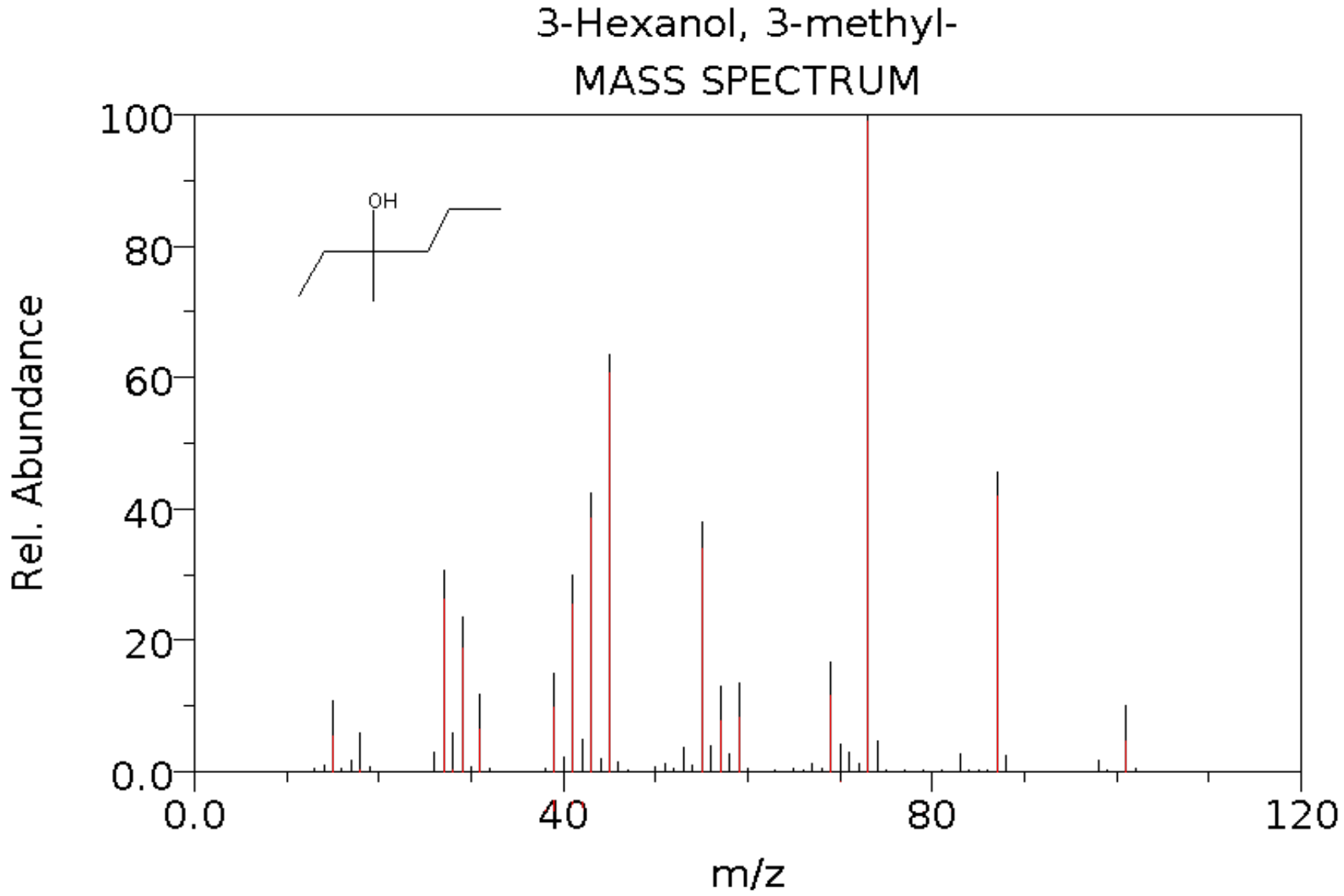

NIST Chemistry WebBook (http://webbook.nist.gov/chemistry)

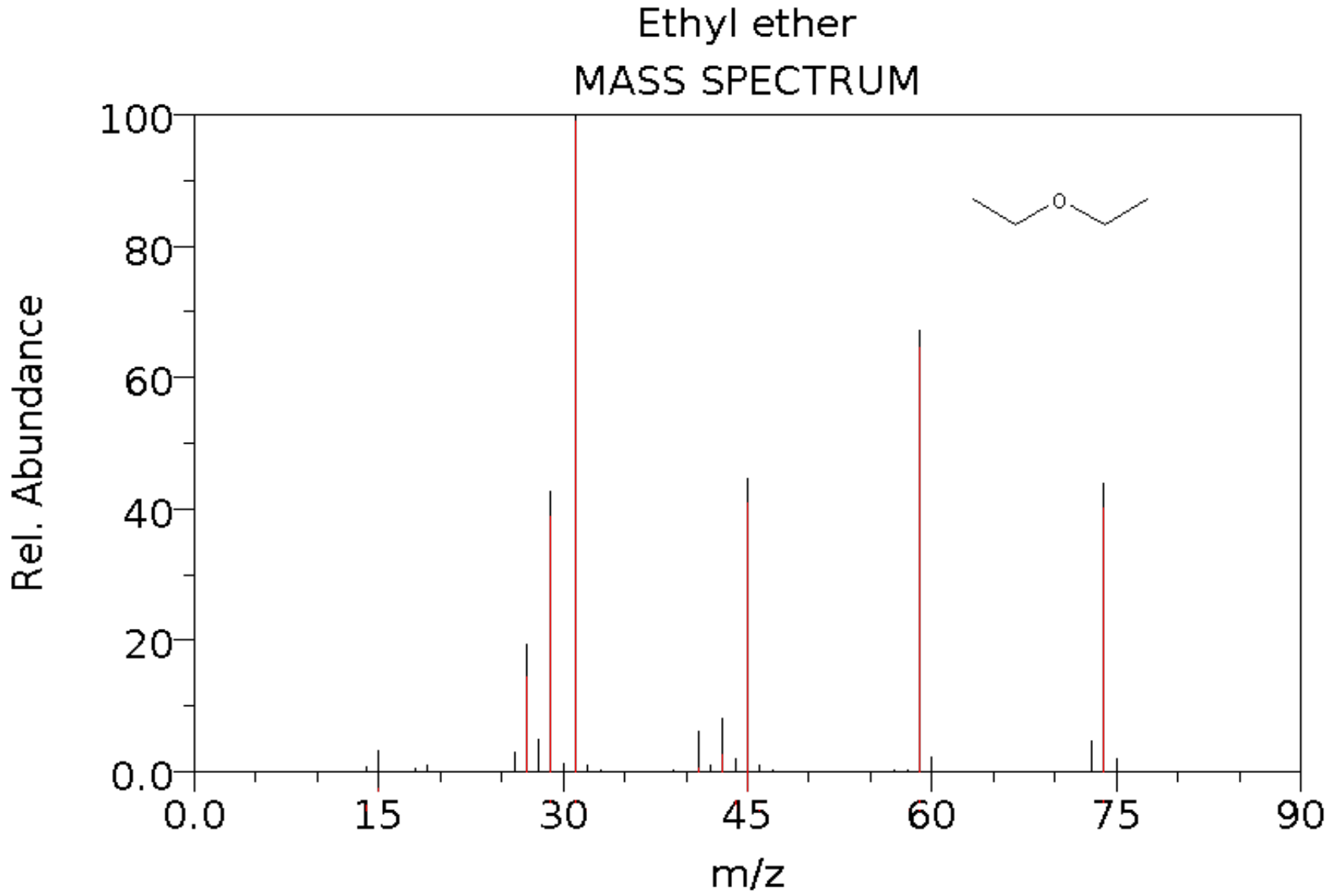

NIST Chemistry WebBook (http://webbook.nist.gov/chemistry)

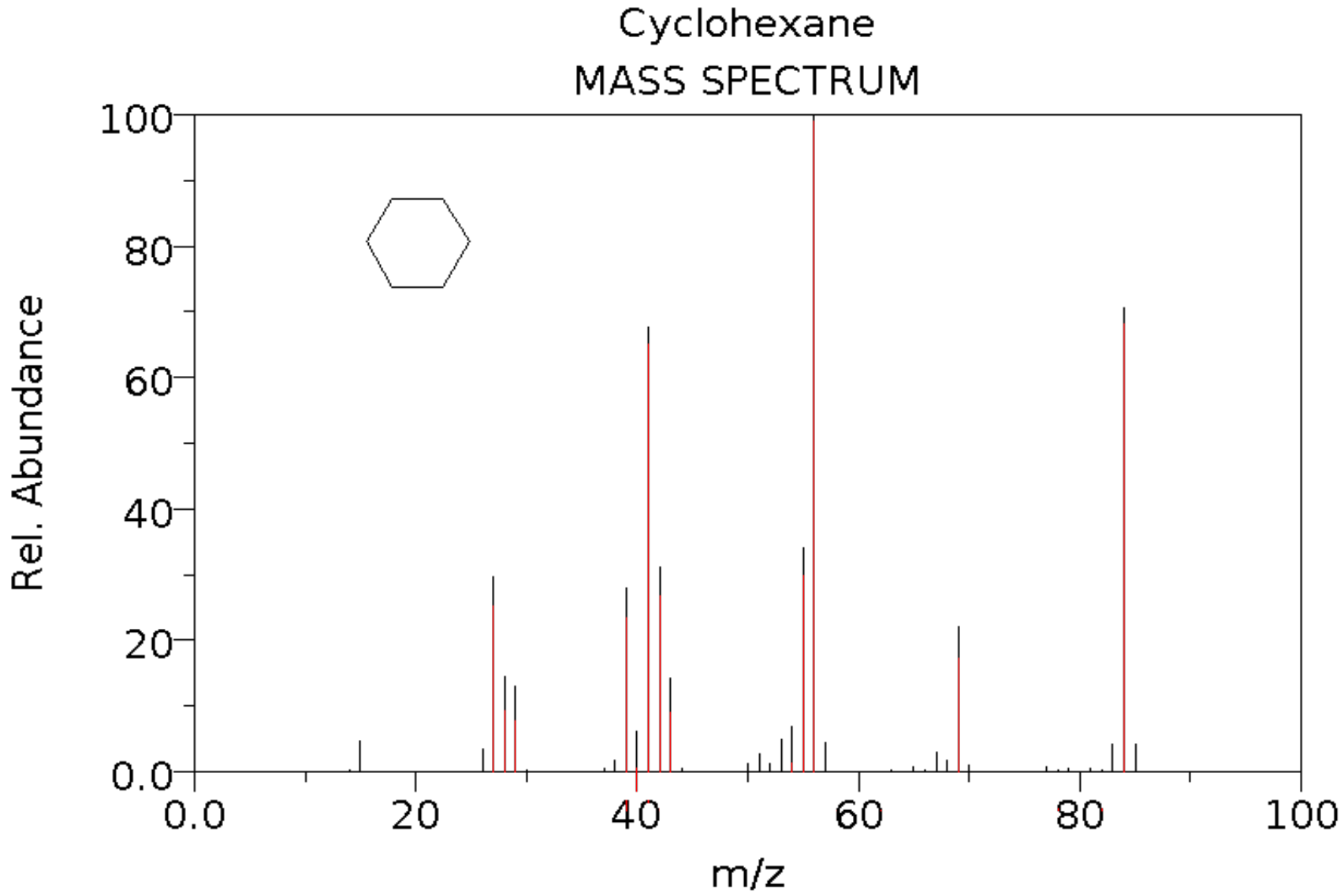

NIST Chemistry WebBook (http://webbook.nist.gov/chemistry)

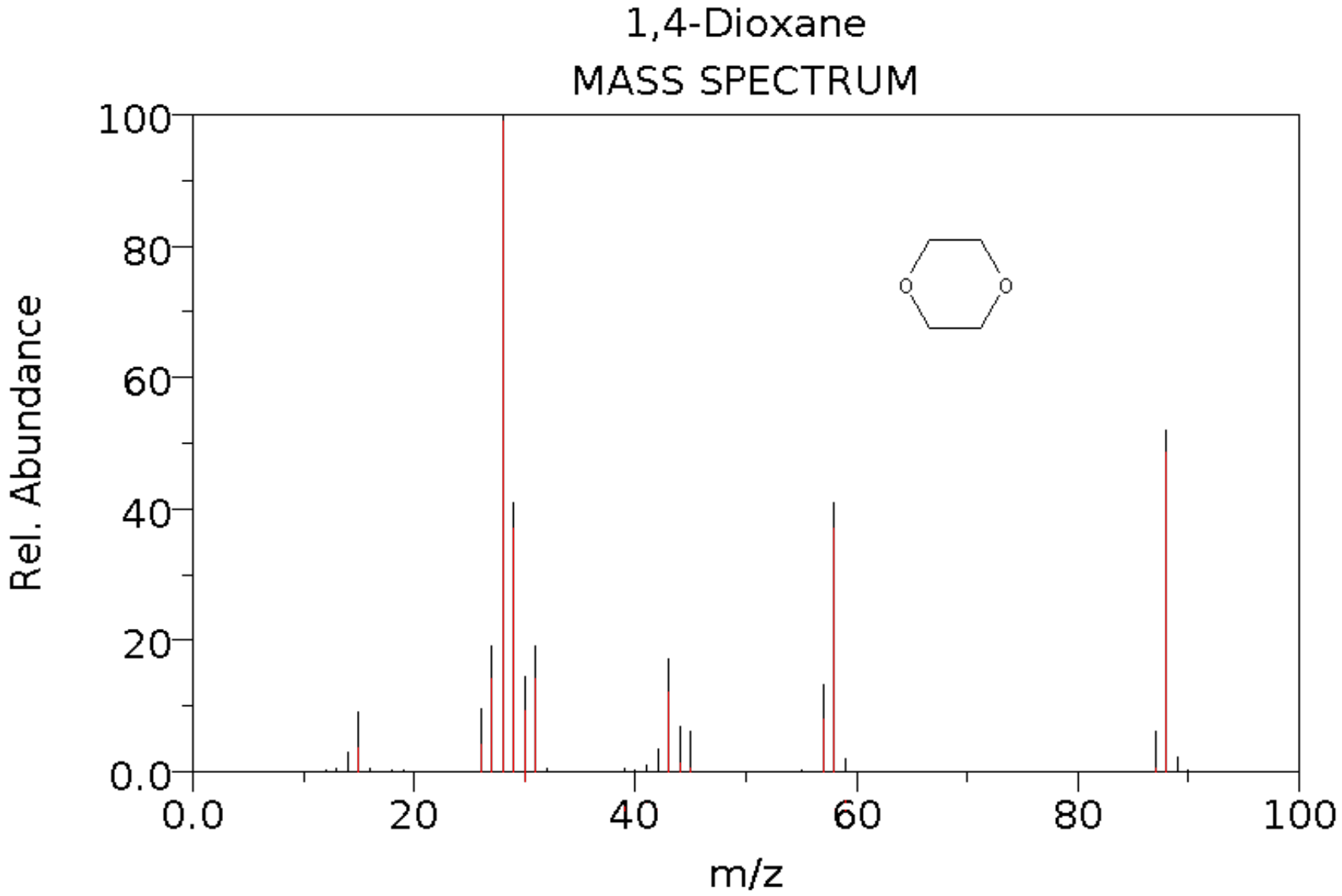
1,4-Dioxane
MASS SPECTRUM
Rel. Abundance
100
80
60
40
20
0.0
0.0
20
40
60
80
100
m/z
NIST Chemistry WebBook (http://webbook.nist.gov/chemistry)

Butylamine, N-methyl-N-propyl-

MASS SPECTRUM

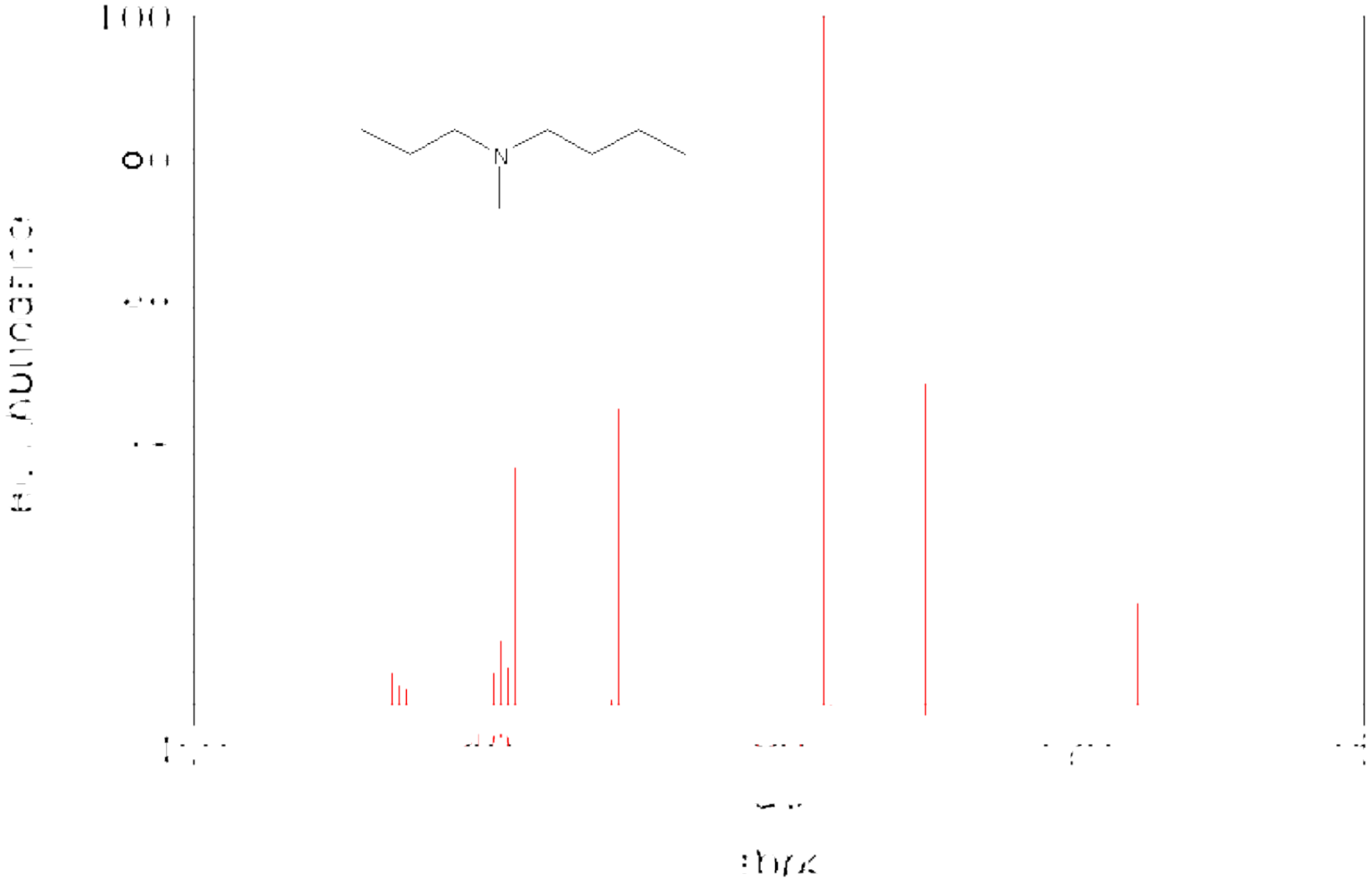

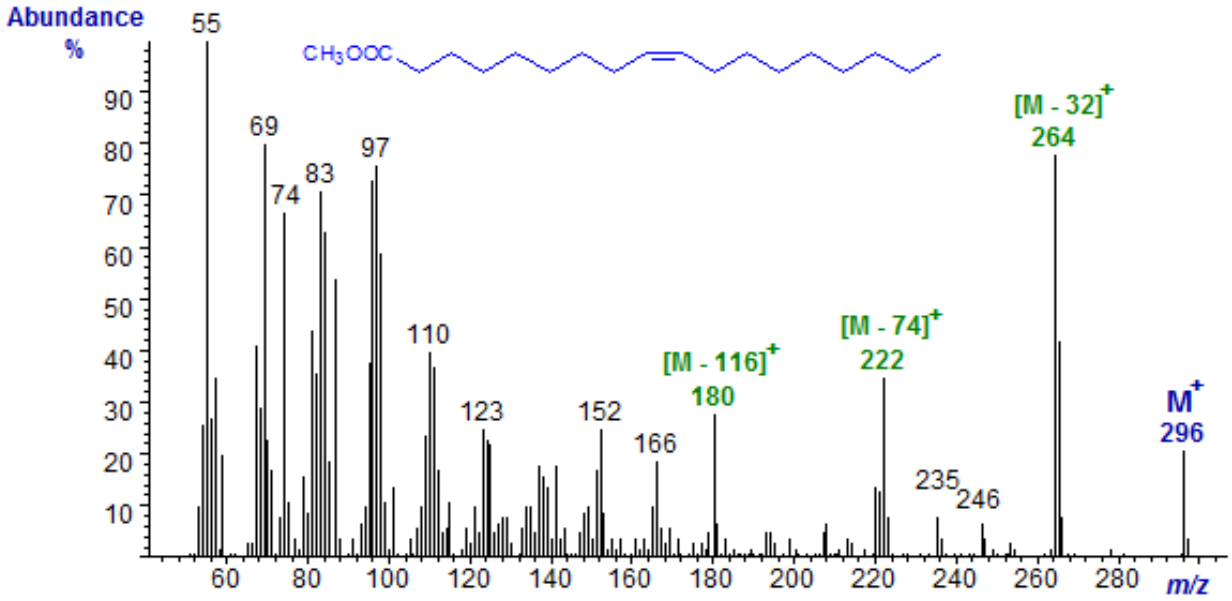
Abundance
%
CH3OOC
55
69
74
83
97
110
123
152
166
[M - 116]+
180
[M - 74]+
222
[M - 32]+
264
M+
296
235
246
m/z

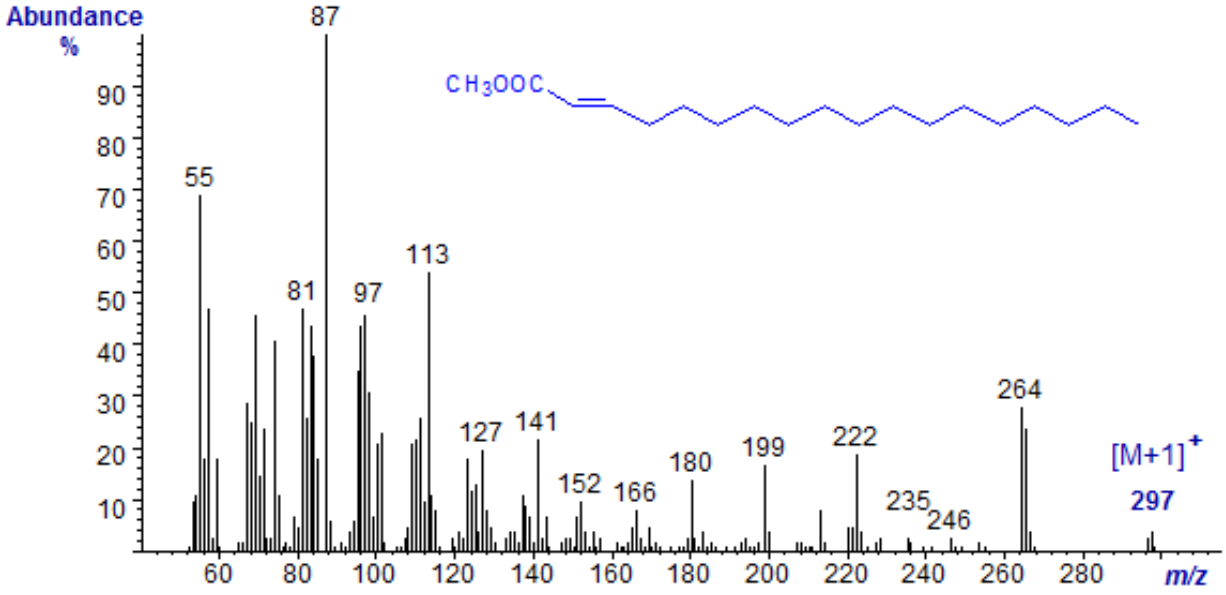
Abundance
%
CH3OOC
87
55
81
97
113
127
141
152
166
180
199
222
235
246
264
[M+1]+
297
m/z

Electrospray/Nanospray Ionization

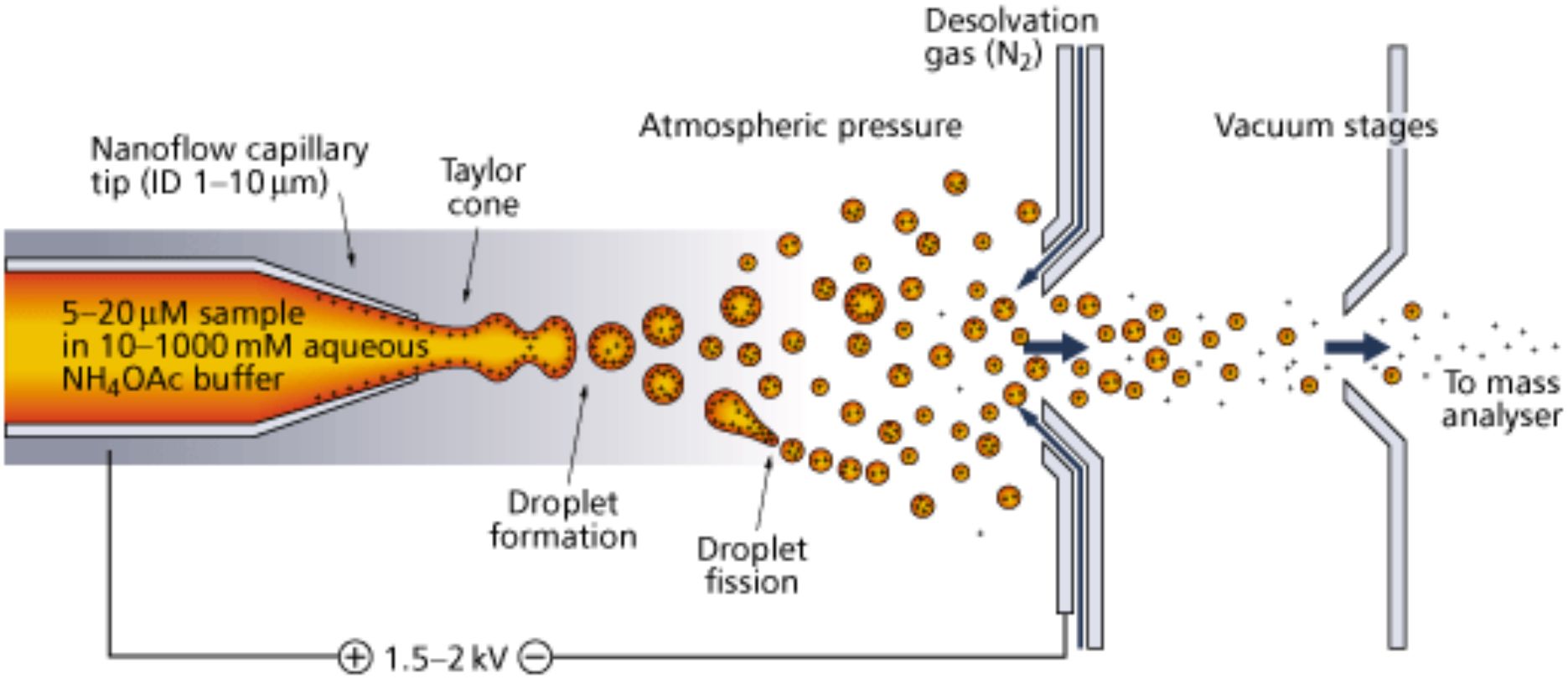

Image from: http://www.uab.edu/botanicals/pdfs/08_Sam090902.pdf

Hitachi M8000 LC/MSn

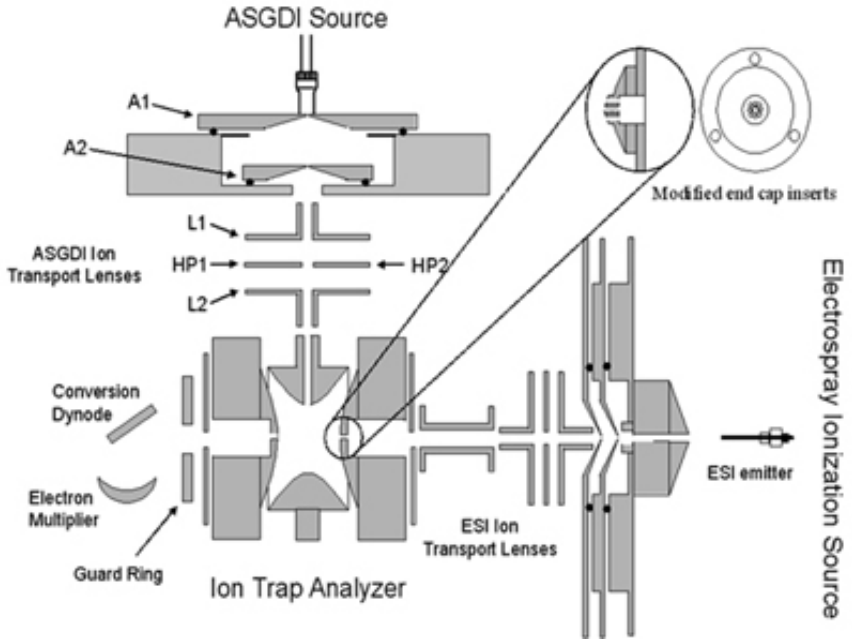

ESI

QStar

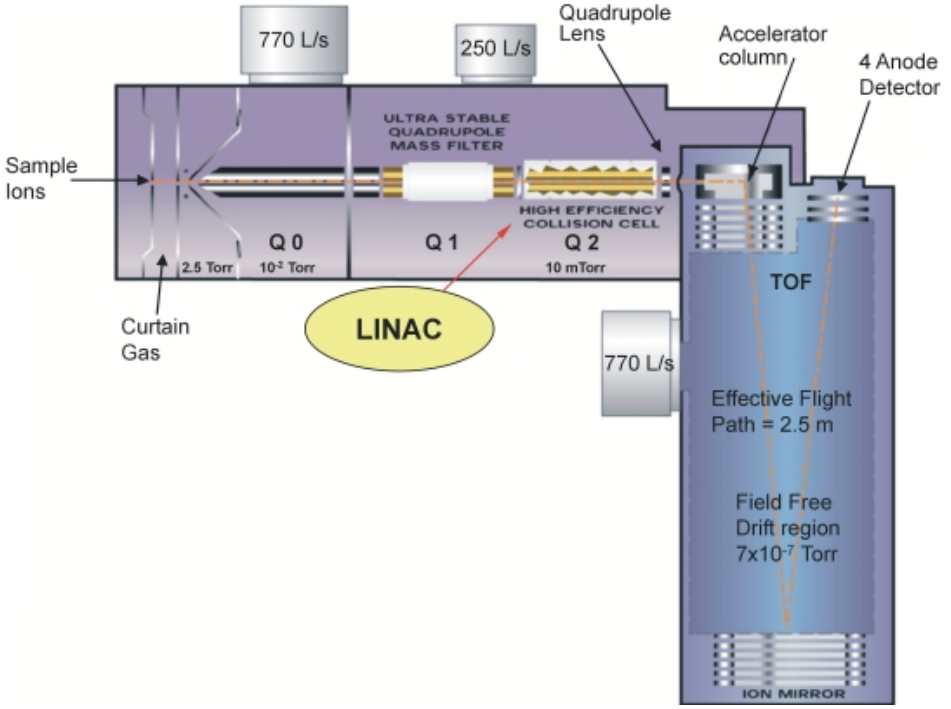

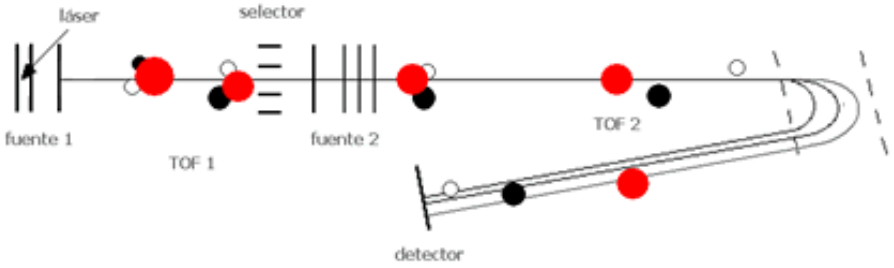

ESI

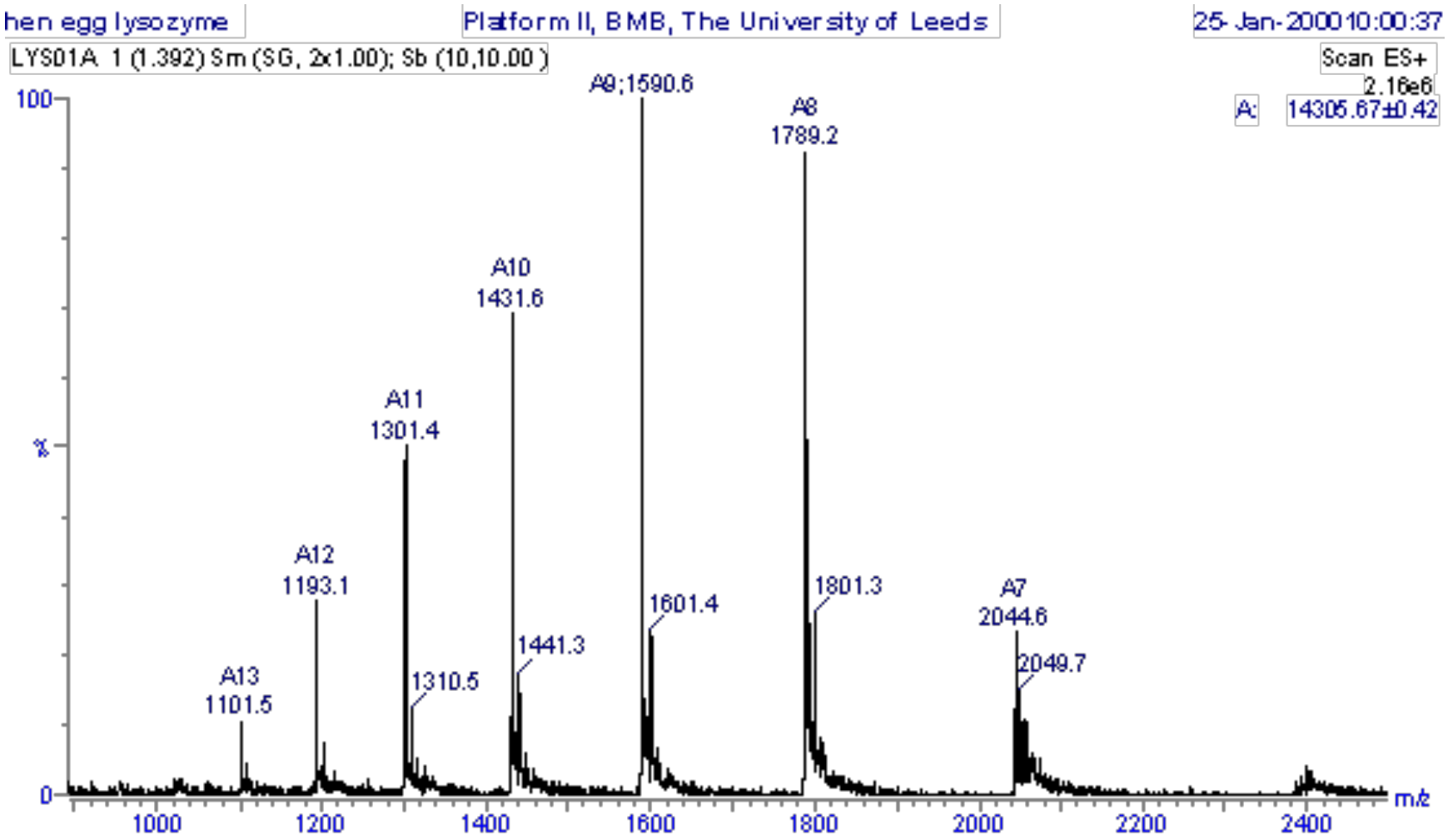
hen egg lysozyme
Platform II, BMB, The University of Leeds
25-Jan-2000 10:00:37
LYS01A 1 (1.392) Sm (SG, 2x1.00); Sb (10,10.00)
Scan ES+
2.16e6
A: 14305.67±0.42
100
%
0
A9;1590.6
A8
1789.2
A10
1431.6
A11
1301.4
A12
1193.1
A13
1101.5
1310.5
1441.3
1601.4
1801.3
A7
2044.6
2049.7
1000
1200
1400
1600
1800
2000
2200
2400
m/z

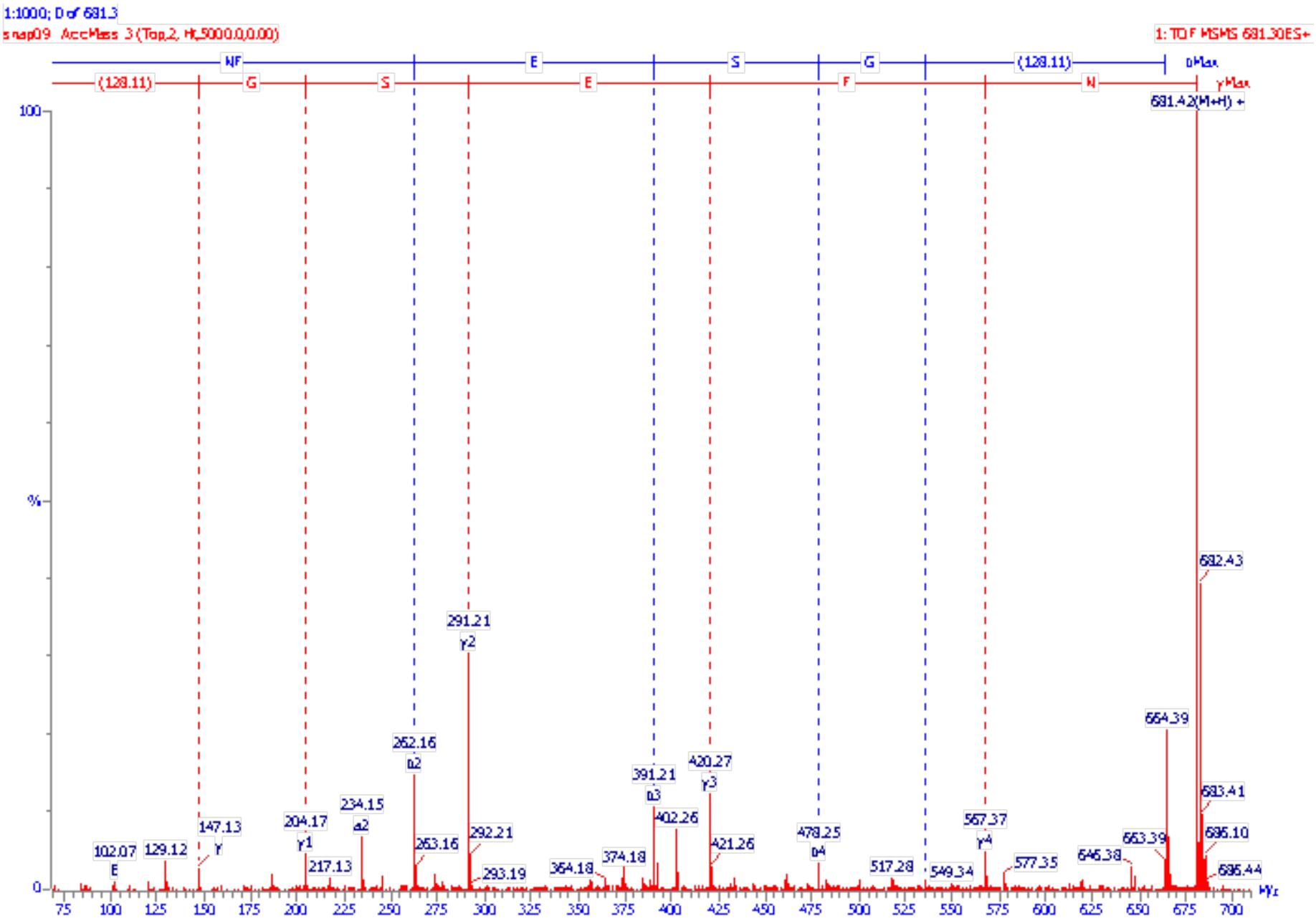
1:1000; D of 681.3
snap09 AccMass 3 (Top,2, Hi,5000.0,0.00)
1: TOF MSMS 681.30 ES+
NF
E
S
G
(128.11)
(128.11)
G
S
E
F
N
bMax
yMax
681.42(M+H) +
100
%
0
682.43
664.39
683.41
696.10
695.44
663.39
646.38
291.21
y2
262.16
b2
420.27
y3
391.21
b3
234.15
a2
204.17
y1
147.13
y
102.07
E
129.12
217.13
263.16
292.21
293.19
364.18
374.18
402.26
421.26
478.25
b4
517.28
549.34
567.37
y4
577.35
75
100
125
150
175
200
225
250
275
300
325
350
375
400
425
450
475
500
525
550
575
600
625
650
675
700
M/z

Amino Acid	3 Letter Code	Single Letter Code		Residue Mass	
				Monoisotopic	Average
Glycine	Gly	G		57.02147	57.052
Alanine	Ala	A		71.03712	71.079
Serine	Ser	S		87.03203	87.078
Proline	Pro	P		97.05277	97.117
Valine	Val	V		99.06842	99.133
Threonine	Thr	T		101.04768	101.105
Cysteine	Cys	C		103.00919	103.144
Isoleucine	Ile	I		113.08407	113.160
Leucine	Leu	L		113.08407	113.160
Asparagine	Asn	N		114.04293	114.104
Aspartic Acid	Asp	D		115.02695	115.089
Glutamine	Gln	Q		128.05858	128.131
Lysine	Lys	K		128.09497	128.174
Glutamic Acid	Glu	E		129.04260	129.116
Methionine	Met	M		131.04049	131.198
Histidine	His	H		137.05891	137.142
Phenylalanine	Phe	F		147.06842	147.177
Arginine	Arg	R		156.10112	156.188
Tyrosine	Tyr	Y		163.06333	163.170
Tryptophan	Try	W		186.07932	186.213
Homoserine Lactone				83.03712	83.090
Homoserine				101.04768	101.105
Pyroglutamic acid				111.03203	111.100
Carboxyamidomethyl Cysteine				160.03065	160.197
Carboxymethylcysteine				161.01466	161.181
Pyridylethylcysteine				208.06703	208.284

Peptide Fragmentation

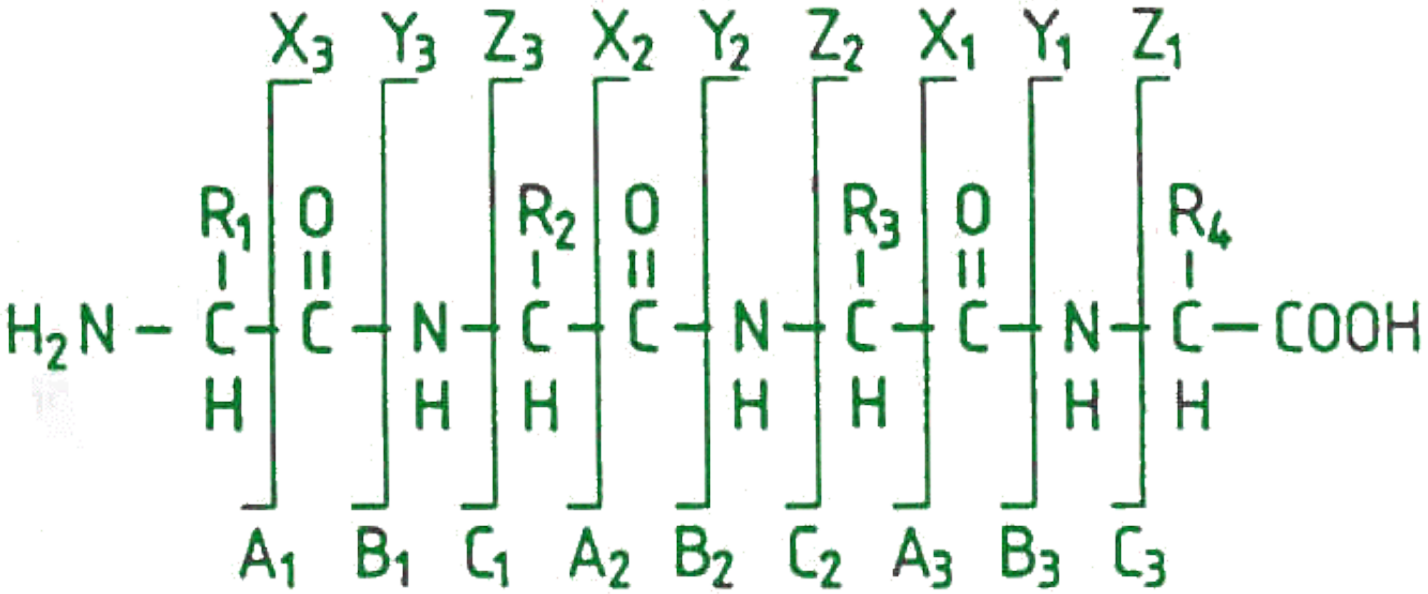

Peptide Fragmentation

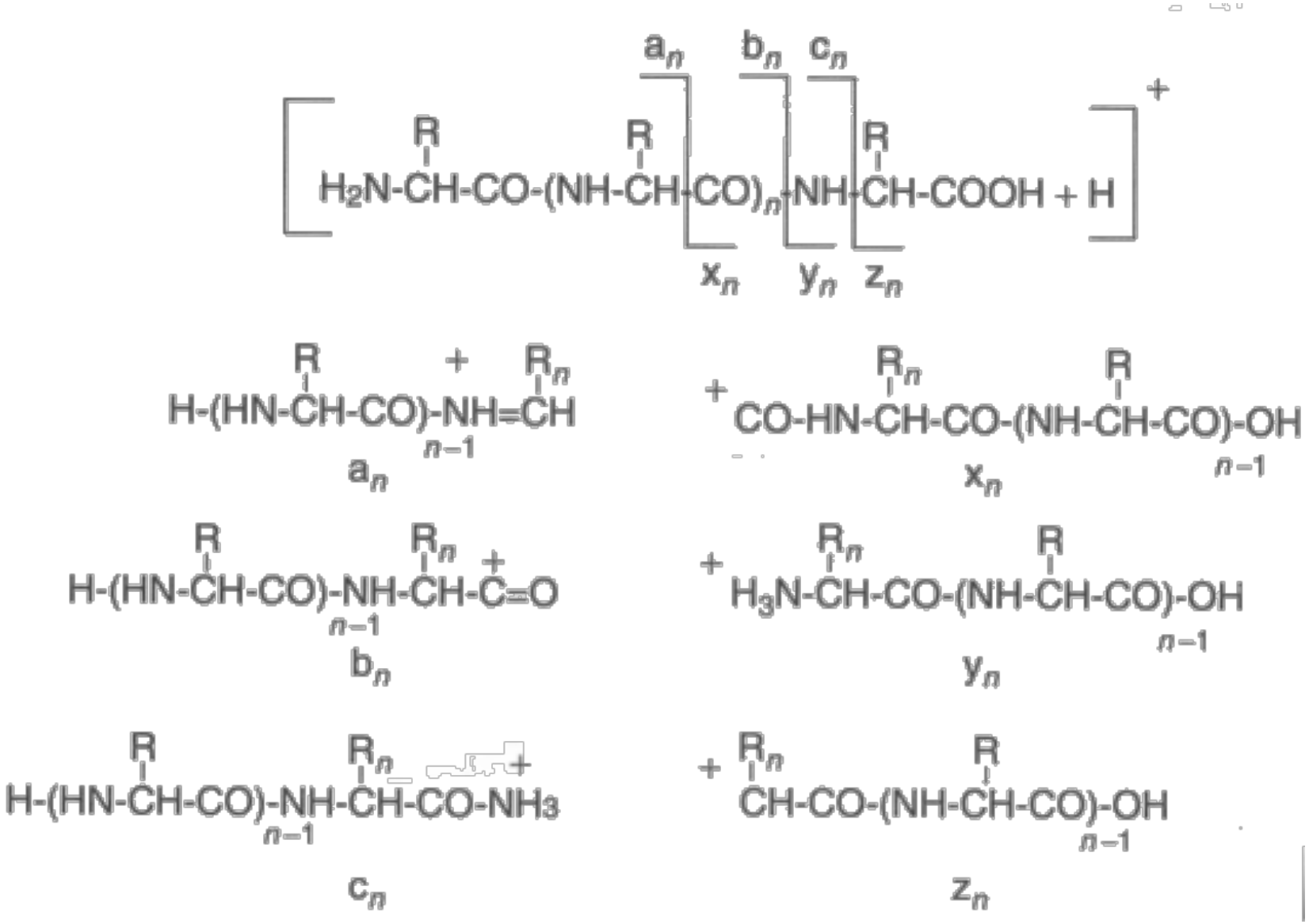

MALDI Ionization

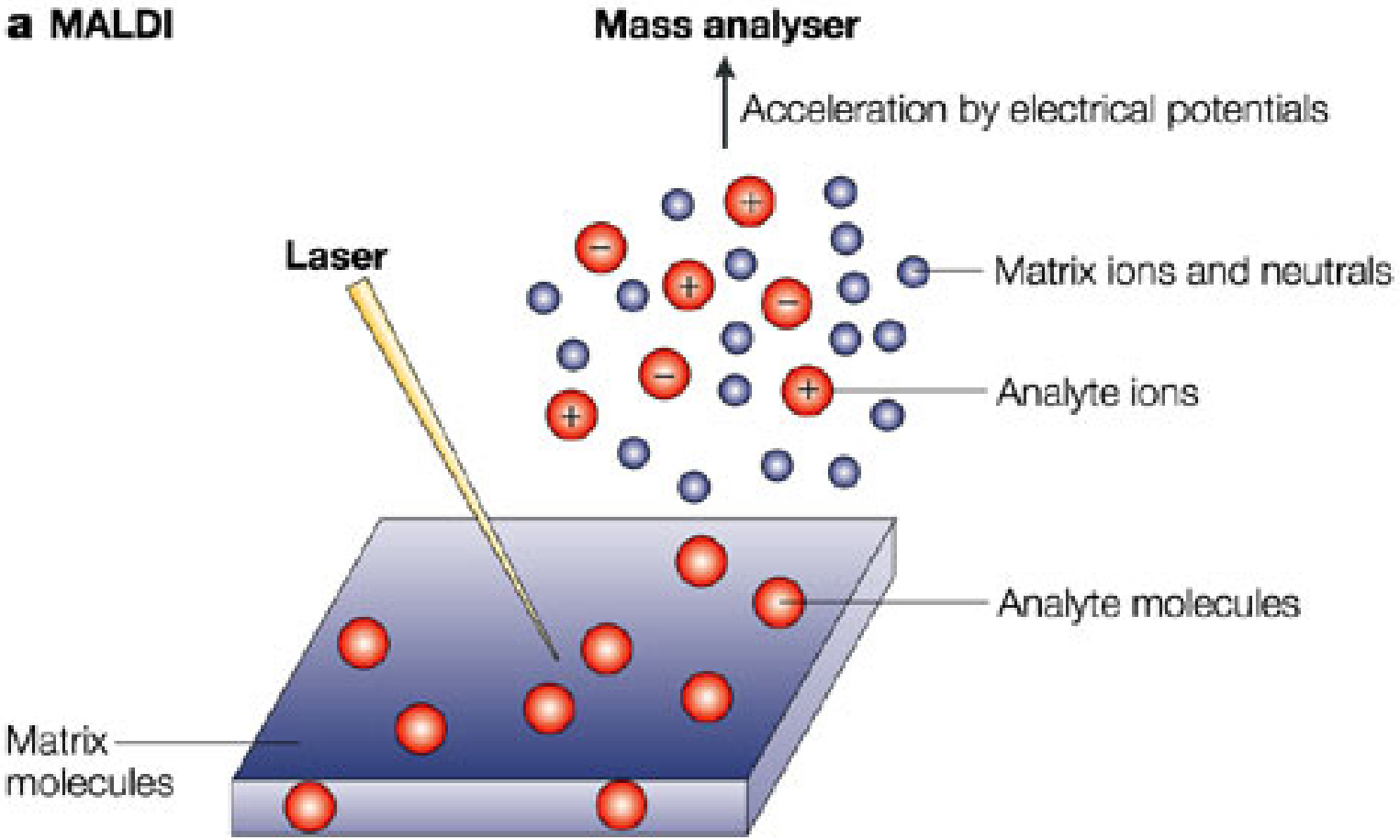

Hanno Steen & Matthias Mann *Nature Reviews Molecular Cell Biology* **2004,** *5*, 699.

Benzoic acid derivatives

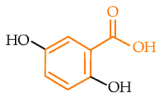

2,5-dihydroxybenzoic acid
(DHB)

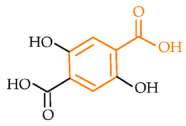

2,5-dihydroxyterephthalic acid

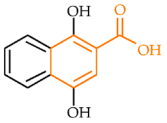

1,4-dihydroxy-2-naphthoic acid

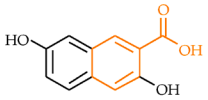

3,7-dihydroxy-2-naphthoic acid

Cinnamic acid derivatives

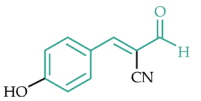

α-cyano-4-hydroxycinnamic acid
(HCCA)

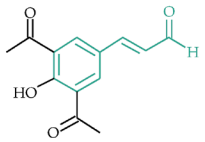

sinapinic acid

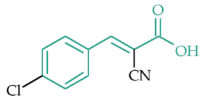

4-chloro-α-cyanocinnamic acid
(ClCCA)

Heterocycles

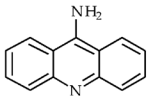

9-aminoacridine (9-AA)

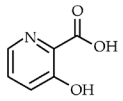

3-hydroxypicolinic acid

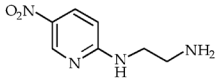

2-(2-aminoethylamino)-5-nitropyridine

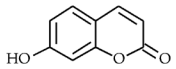

7-hydroxycoumarin

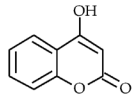

4-hydroxycoumarin

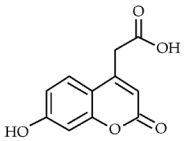

7-hydroxycoumarin-4-acetic acid

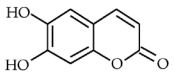

6,7-dihydroxycoumarin
(aesculetin)

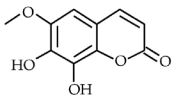

7,8-hydroxy-6-methhoxycoumarin

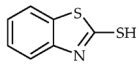

2-mercaptobenzothiazole

Other matrices

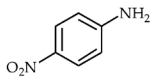

4-nitroaniline
(PNA)

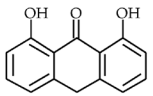

dithranol

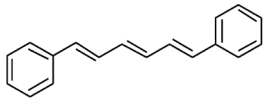

1,6-diphenyl-1,3,5-hexatriene
(DPH)

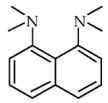

1,8-bis(dimethylamino)naphthalene
(DMAN)

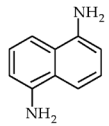

1,5-diaminonaphthalene
(1,5-DAN)

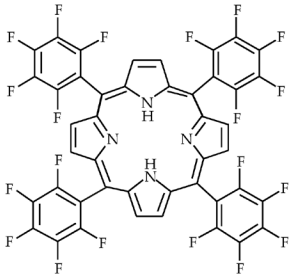

meso-tetratkis(pentafluorophenyl)-
porphyrin

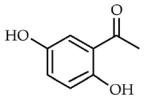

2,5-dihydroxyacetophenone
(2,5-DHAP)

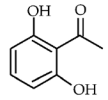

2,6-dihydroxyacetophenone
(2,6-DHAP)

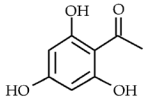

2,4,6-trihydroxyacetophenone
(THAP)

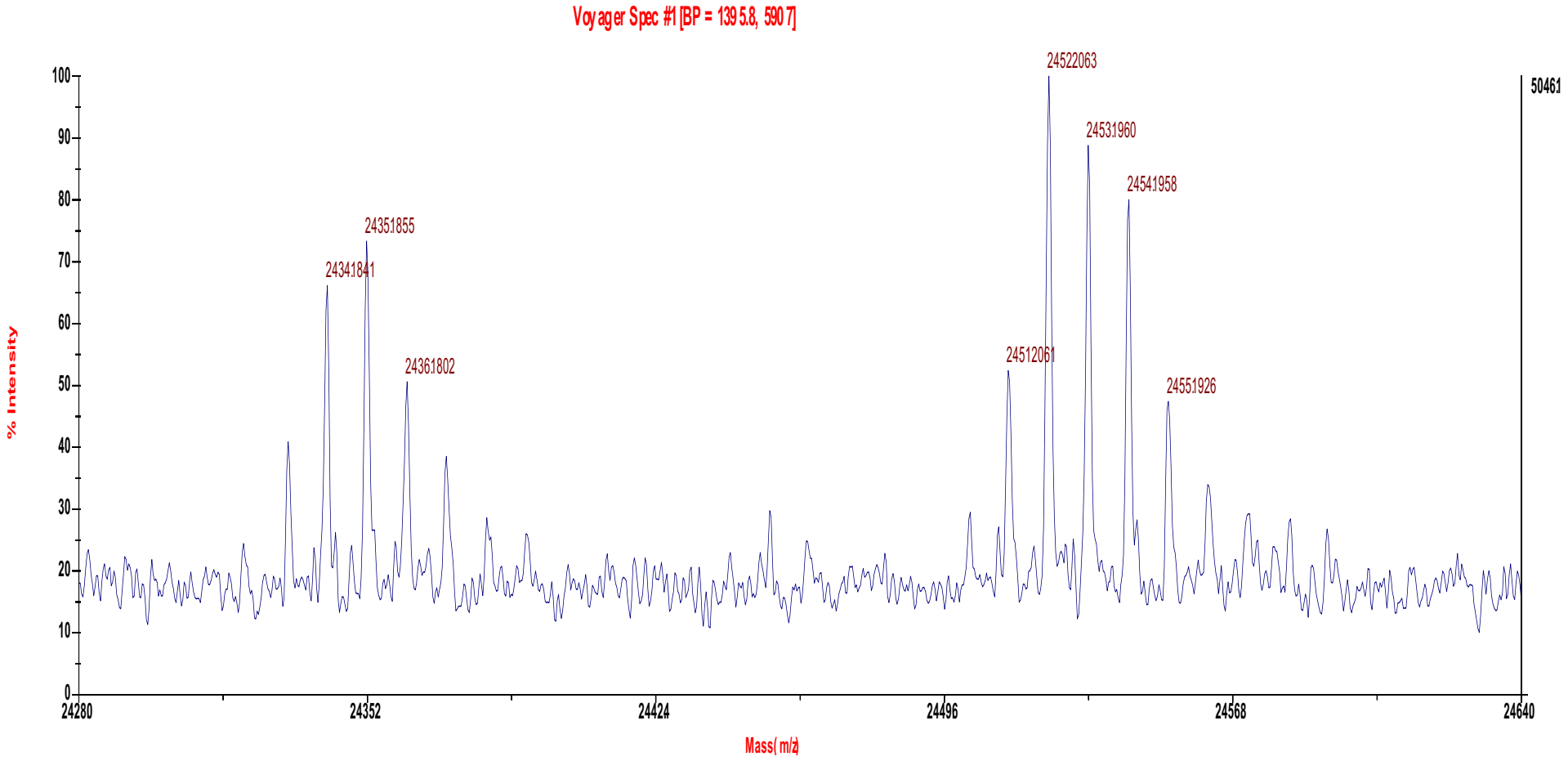
Voyager Spec #1 [BP = 1395.8, 5907]
% Intensity
Mass(m/z)
24341841
24351855
24361802
24512061
24522063
24531960
24541958
24551926
50461
100
90
80
70
60
50
40
30
20
10
0
24280
24352
24424
24496
24568
24640

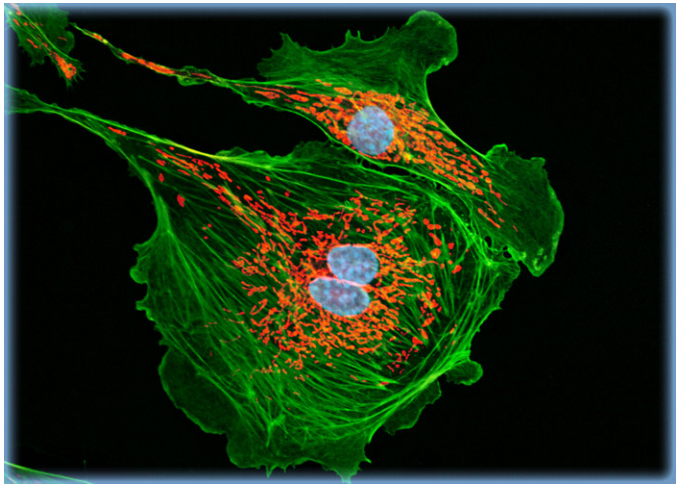

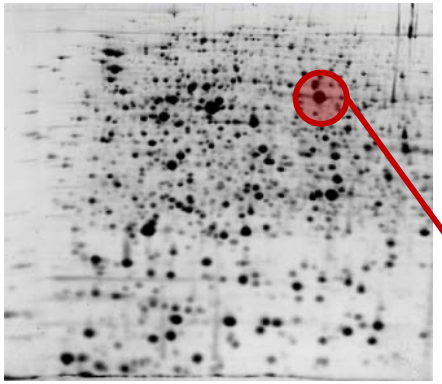

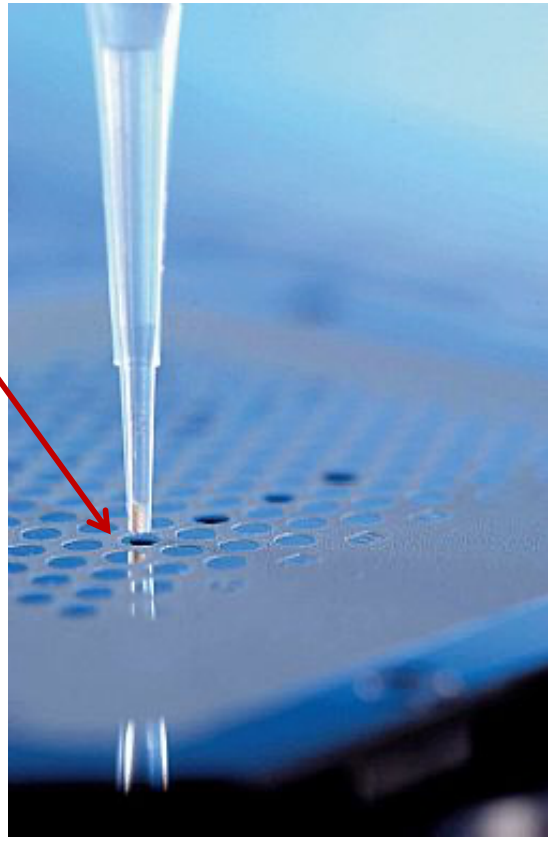

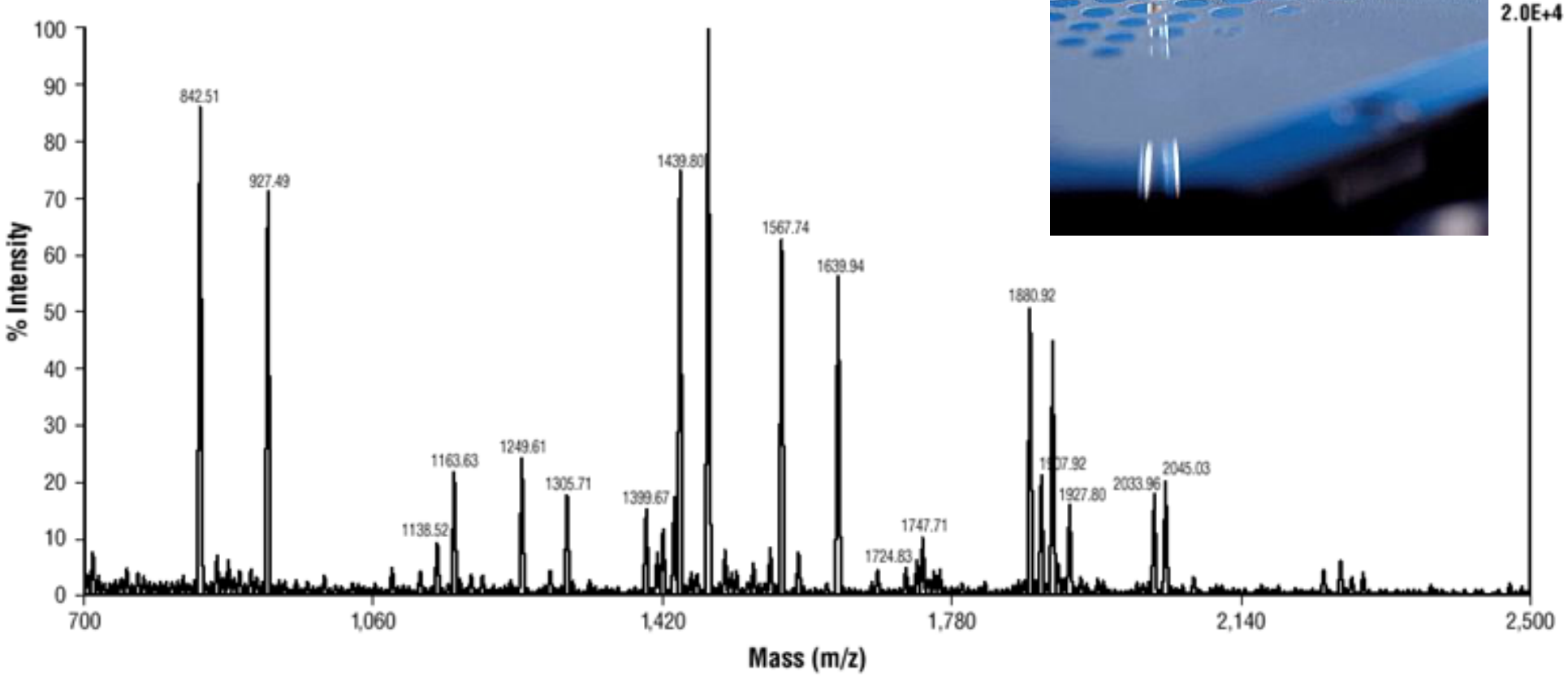
% Intensity
Mass (m/z)
2.0E+4
100
90
80
70
60
50
40
30
20
10
0
700
1,060
1,420
1,780
2,140
2,500
842.51
927.49
1439.80
1567.74
1639.94
1880.92
1163.63
1249.61
1305.71
1138.52
1399.67
1747.71
1724.83
1927.80
2033.96
2045.03

ProteinProspector

v 5.10.0

Proteomics tools for mining sequence databases in conjunction with Mass Spectrometry experiments.

Click here to see the latest new features.

The iPRG2012 study on detecting modified peptides in a complex mixture has been launched!
Click for more details.

ProteinProspector Asia Pacific

ProteinProspector Tools

Batch MSMS Database Searching

Instructions

Search Compare | Batch-Tag Web | Batch-Tag

Results Management | Search Table

Database Search Programs

MS-Fit | MS-Tag | MS-Homology | MS-Bridge

MS-Fit Upload | MS-Seq | MS-Pattern | MS-NonSpecific

Peptide / Protein MS Utility Programs

MS-Digest | MS-Product | MS-Viewer (Video)

MS-Isotope | MS-Comp

Database Management

DB-Stat

Administration/Help

Video Tutorials NEW!
Administering ProteinProspector
User's Manual
FAQ
Bug Listing
ProteinProspector Revision History
ProteinProspector Automation Guidance

Useful Tables

- Mutation Mass Shifts
- Dipeptide Masses
- Trypsin Autolysis Products

Publications
Useful Links

Questions/comments email: ppadmin@cgl.ucsf.edu

These programs were developed in the UCSF Mass Spectrometry Facility, which is directed by Dr. Alma Burlingame, Professor of Chemistry an and funded by the NIH National Center for Research Resources.

MS-Fit

Database: User Protein; NCBInr.2011.10.10; NCBInr.2011.10.10.random; NCBInr.2011.10.10.random.concat

[+] User Protein Sequence

DNA Frame Translation: 3

Taxonomy: All; HUMAN MOUSE; HUMAN RODENT; MODEL PLANTS; RODENT; ROACH LOCUST BEETLE

Output: HTML | Hits to file: ☐ | Name: lastres

Digest: Trypsin | Max. Missed Cleavages: 1

Constant Mods: Acetohydrazide (C-term); Acetohydrazide (DE); Acetyl (K); Acetyl (N-term); Acetyl:2H(3) (K); Acetyl:2H(3) (N-term)

[+] Pre-Search Parameters

Start Search

Sample ID (comment):

Display Graph: ☐

Maximum Reported Hits: 5

Sort By: Score Sort

Report Homologous Proteins: Interesting

Min. # peptides required to match: 4

Report MOWSE Scores: ☑ Pfactor: 0.4

Masses are: monoisotopic

Tol: 20 ppm | Sys Err: 0

Contaminant Masses:

Possible Modifications: Peptide N-terminal Gln to pyroGlu; Oxidation of M; Protein N-terminus Acetylated; Acrylamide Modified Cys

User Def Mod 1: Acetyl (K)

User Def Mod 2: Acetyl (K)

User Def Mod 3: Acetyl (K)

User Def Mod 4: Acetyl (K)

OR

Unknown Amino Acid: ☐ Single Base Change: ☐ Homology: ☐

Max Mods: 1 Min. # match with NO AA subs: 1

Instrument: ESI-Q-TOF | Data Format: PP M/Z Charge

Data Paste Area

```
842.5100
856.5220
864.4733
870.5317
940.4754
943.4885
959.4934
970.4308
```

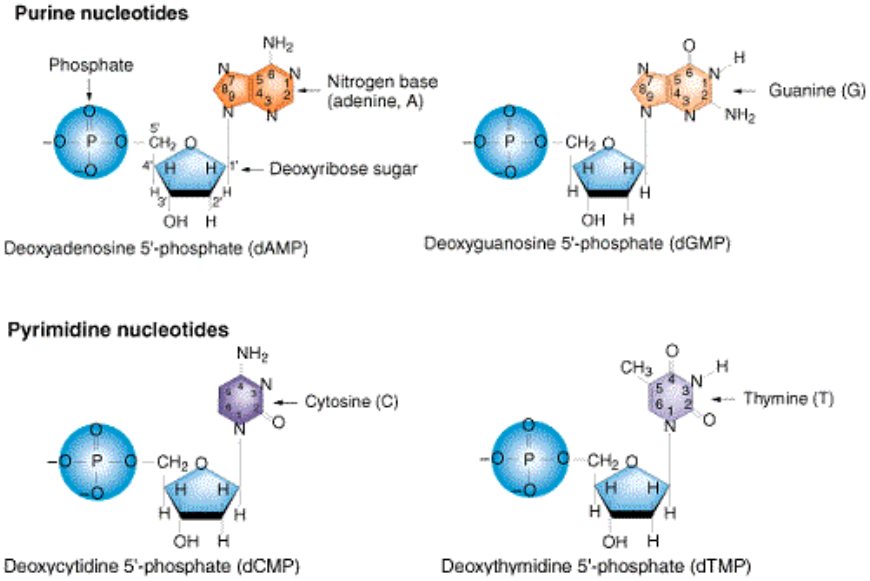

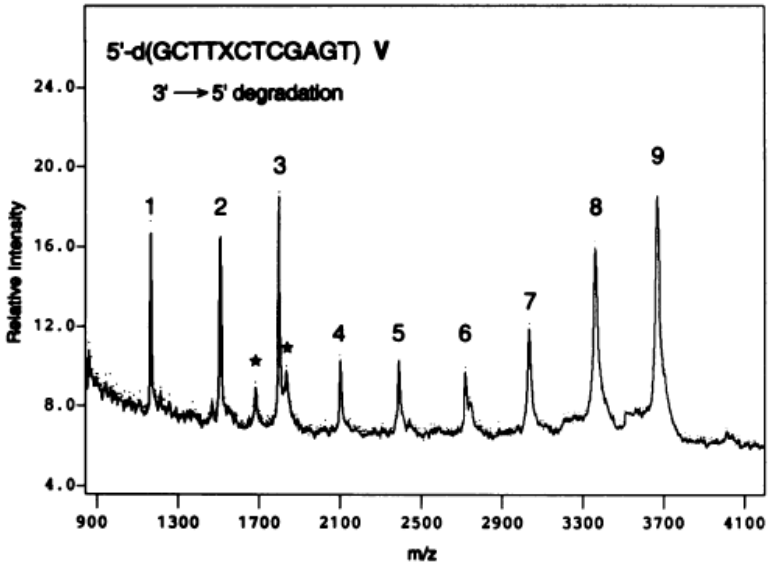

Peak	Sequence	Mass calc.	Mass *found*	Δm
1	5'-d(GCTT)	1163.8	*1163.9*	-0.1
2	5'-d(GCTTX)	1507.1	*1506.9*	0.2
3	5'-d(GCTTXC)	1796.2	*1796.2*	0
4	5'-d(GCTTXCT)	2100.4	*2100.5*	-0.1
5	5'-d(GCTTXCTC)	2389.6	*2389.8*	-0.2
6	5'-d(GCTTXCTCG)	2718.9	*2719.3*	-0.4
7	5'-d(GCTTXCTCGA)	3032.1	*3032.8*	-0.7
8	5'-d(GCTTXCTCGAG)	3361.3	*3362.0*	-0.7
9	5'-d(GCTTXCTCGAGT)	3665.5	*3666.0*	-0.5

Nucleic Acids Research, 1993, Vol. 21, No. 14 3195

Ion Beam Sputtering

- The bombarding primary ion beam produces monatomic and polyatomic particles of sample material and resputtered primary ions, along with electrons and photons.
- The secondary particles carry negative, positive, and neutral charges and they have kinetic energies that range from zero to several hundred eV.
- Primary beam: Cs+, O2+, O , Ar+, and Ga+ with depths of depths 1 to 10 nm between 1 and 30 keV.

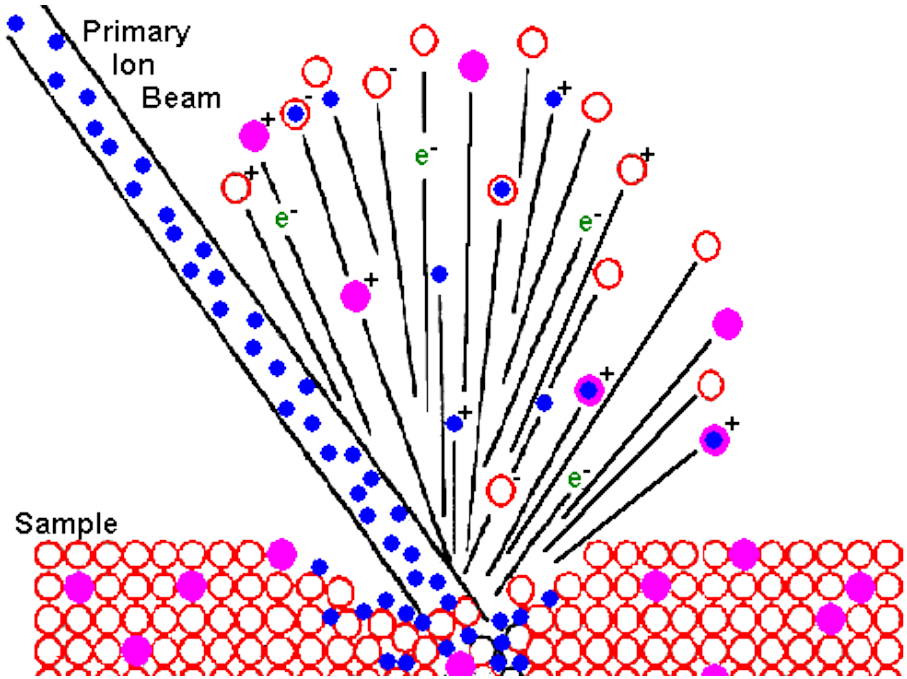

Sputtering Effects

- The collision cascade model has the best success at quantitatively explaining how the primary beam interacts with the sample atoms.
- Sputtering leads to surface roughness in the sputter craters.

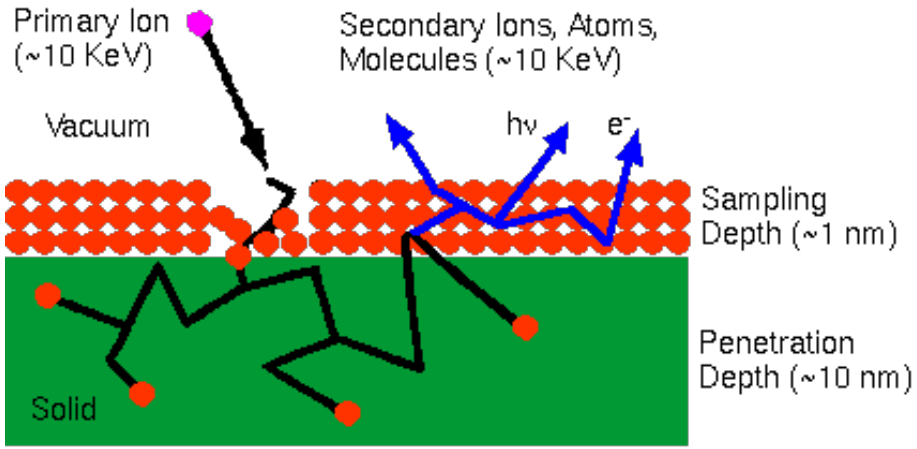

Secondary Ion Energy Distributions

- The sputtering process produces secondary ions with a range of (translational) kinetic energies.
- Molecular Ions (internal vibrational and rotational modes)
- Atomic Ions (only in translational modes)

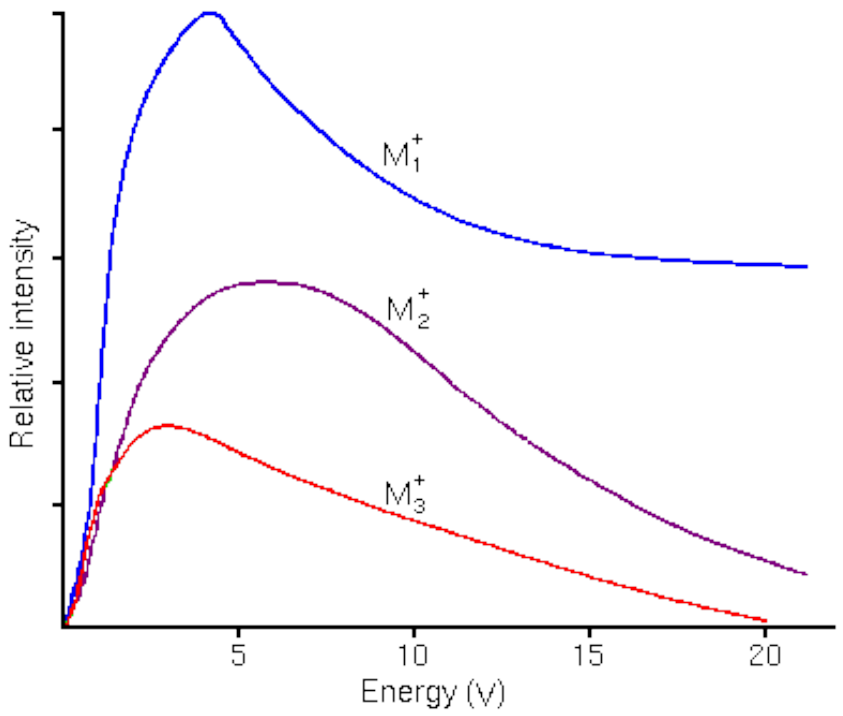

Secondary Ion Yields
Primary Beam Effects

- The variability in ionization efficiencies leads to different analysis conditions for different elements as indicated on the periodic table.

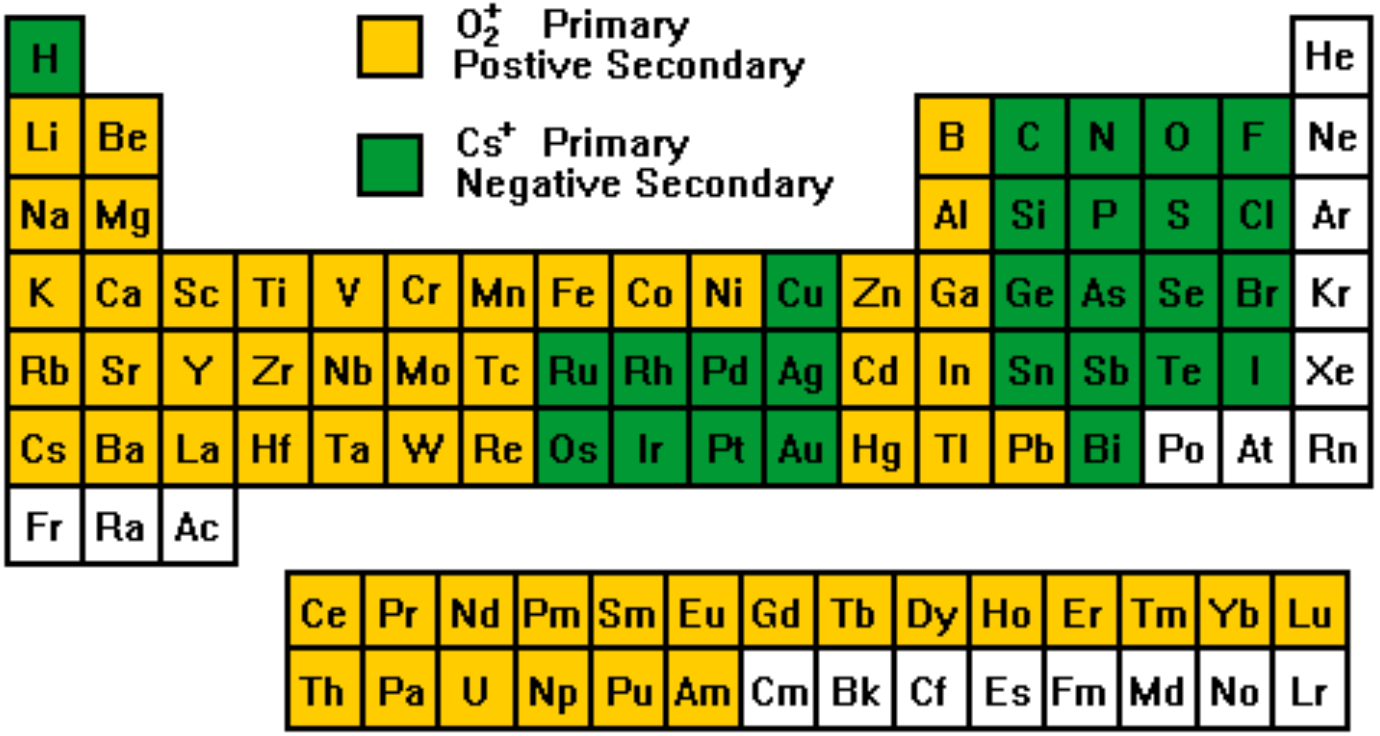

Sensitivity and Detection Limits

- The SIMS detection limits for most trace elements are between $1x10^{12}$ and $1x10^{16}$ atoms/cc.
- Dark Current : The output of an electron multiplier if no secondary ions are striking it.
- Oxygen present in vacuum systems or analyte atoms sputtered from mass spectrometer parts.

(3) Depth Profiling

- In contrast to a static SIMS experiment, high primary ion dose densities are applied giving a successive removal (sputtering) of the respective top surface layers. By acquiring spectra during the sputtering the in-depth distribution of elements and small clusters (e.g. oxides) can be monitored.

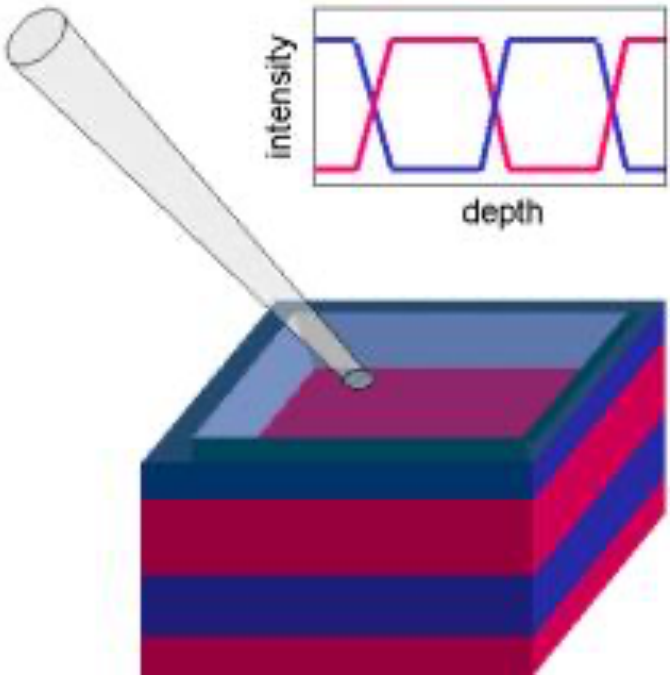

Depth Profiling

- Monitoring the secondary ion count rate of selected elements as a function of time leads to depth profiles.

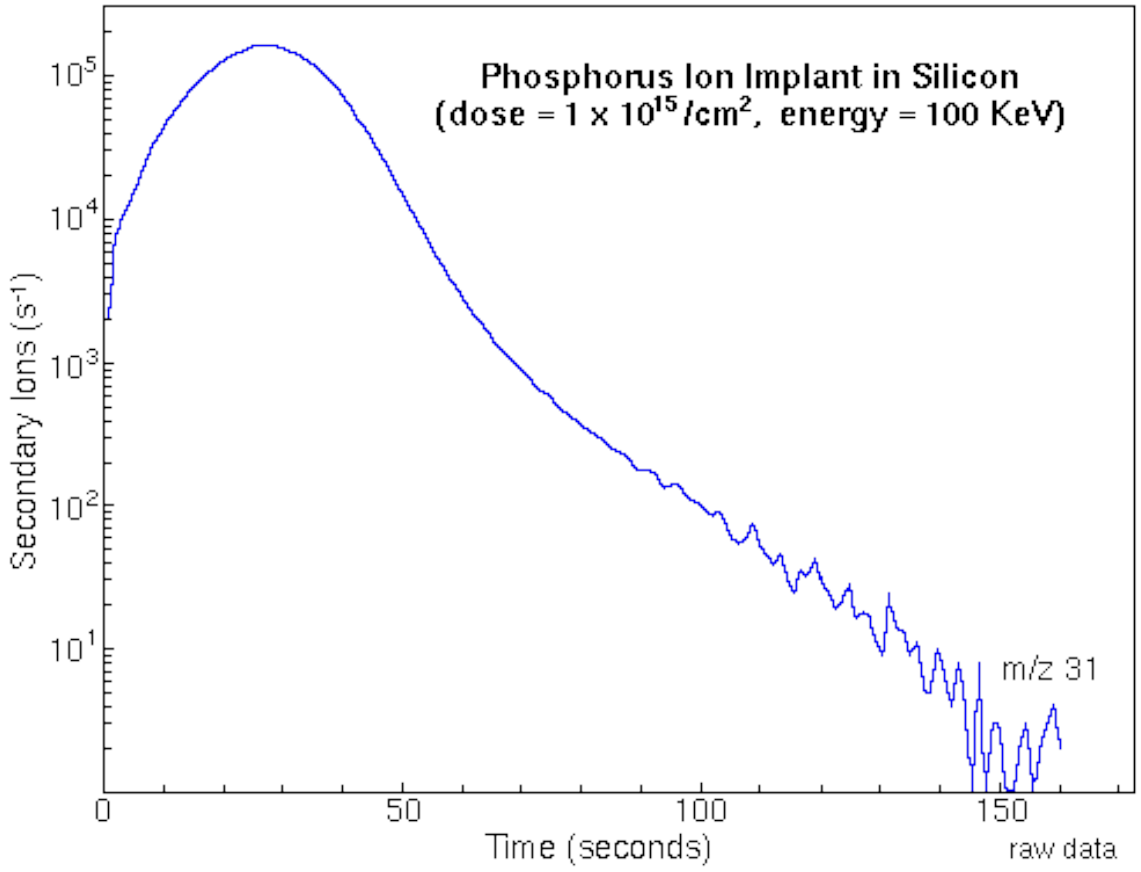

(2) Surface Imaging

- By rastering a finely focussed ion beam over the surface, like an electron beam in an electron microprobe, mass resolved secondary ion images (chemical maps) can be obtained simultaneously.

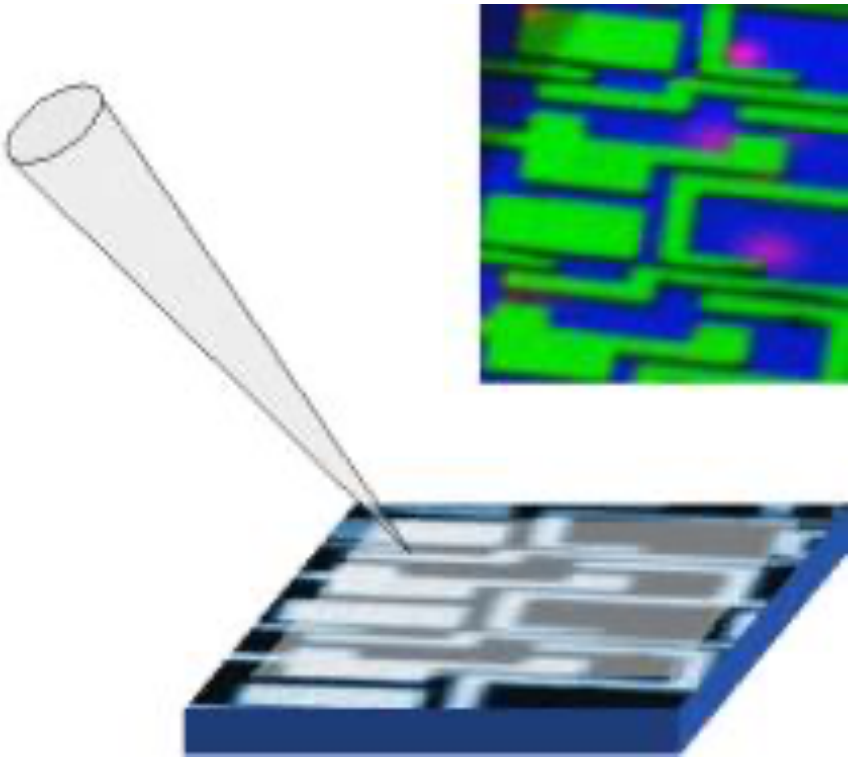

Microbeam Imaging

- For ion microbeam imaging, a finely focused primary ion beam sweeps the sample in a raster pattern and software saves secondary ion intensities as a function of beam position.

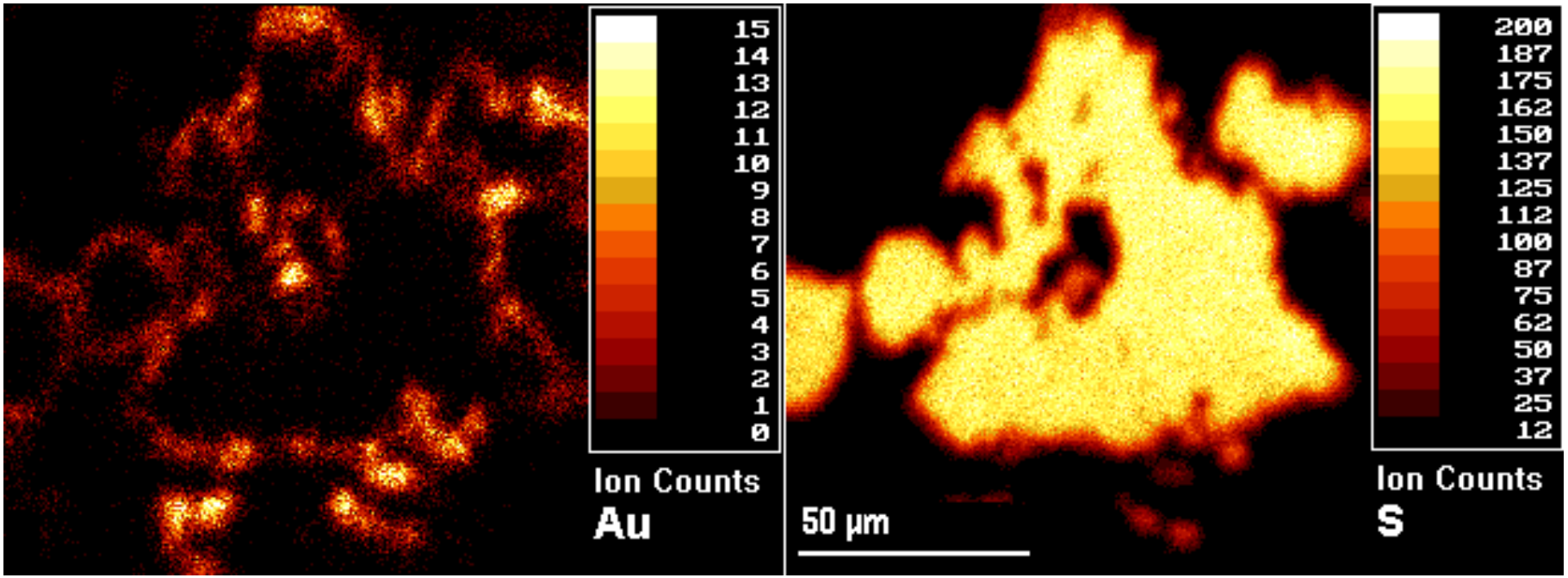

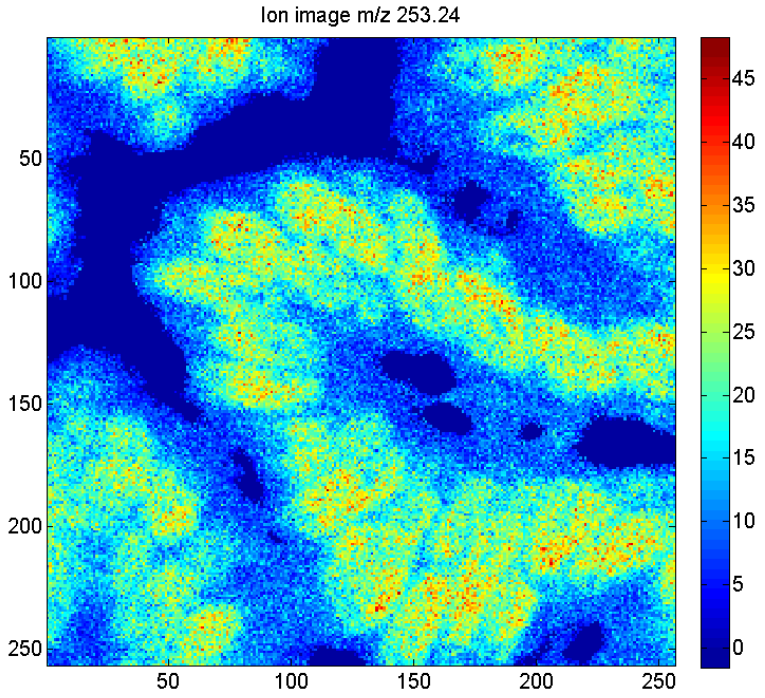

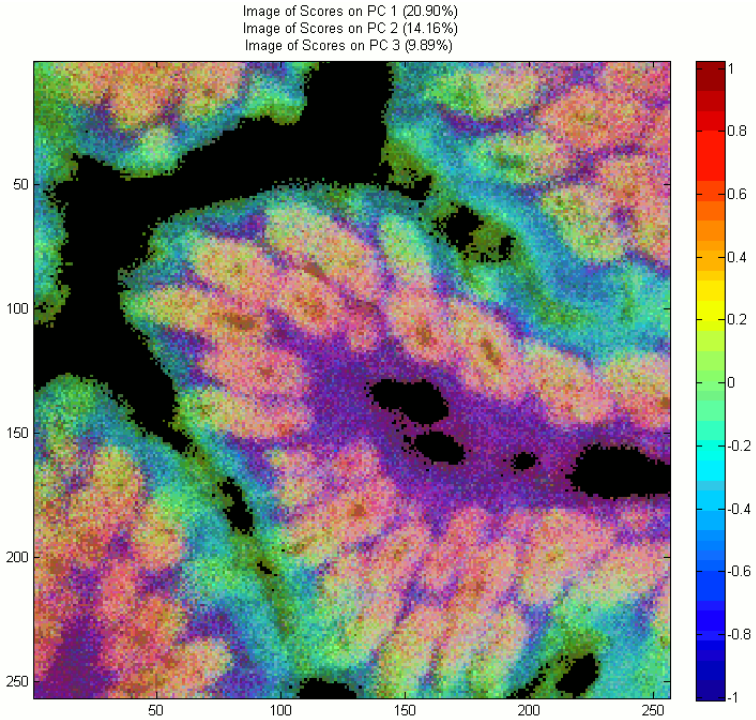

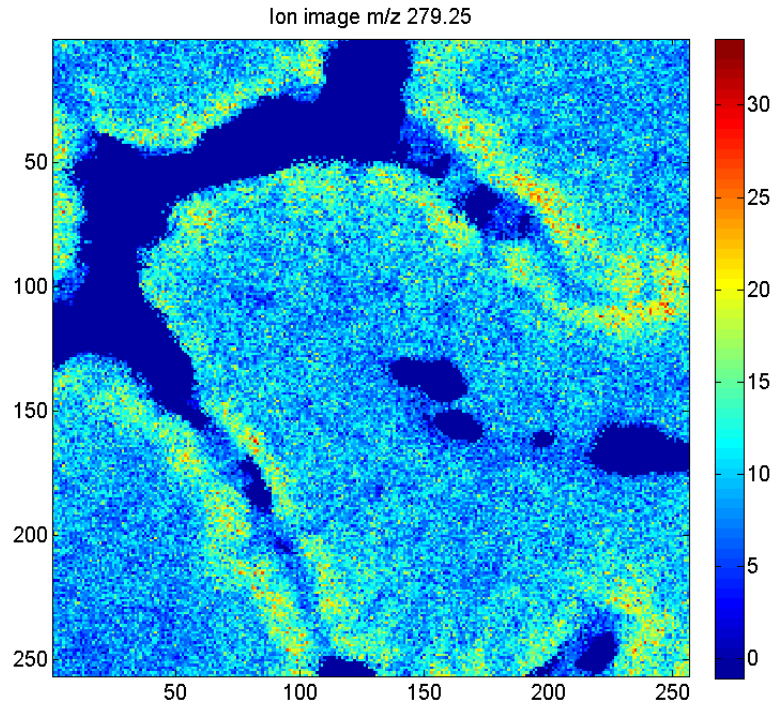

Lipid mapping of colonic mucosa by cluster TOF-SIMS imaging and multivariate analysis in *cftr* knockout mice.

Marc Brulet , 1, * Alexandre Seyer , 1, * Aleksander Edelman , † Alain Brunelle , * Janine Fritsch , † Mario Ollero , 2, * ,† and Olivier Laprévote * , § ***Journal of Lipid Research*, 51 (2010) 3034.**

Building Blocks of An ICP - MS

- Atmospheric pressure
  - Sample introduction
  - Desolvation
  - Atomization
  - Ionization > 90%
- ---------- ----------
- Vacuum
  - Ion focusing
  - Mass separation
  - Isotope detection

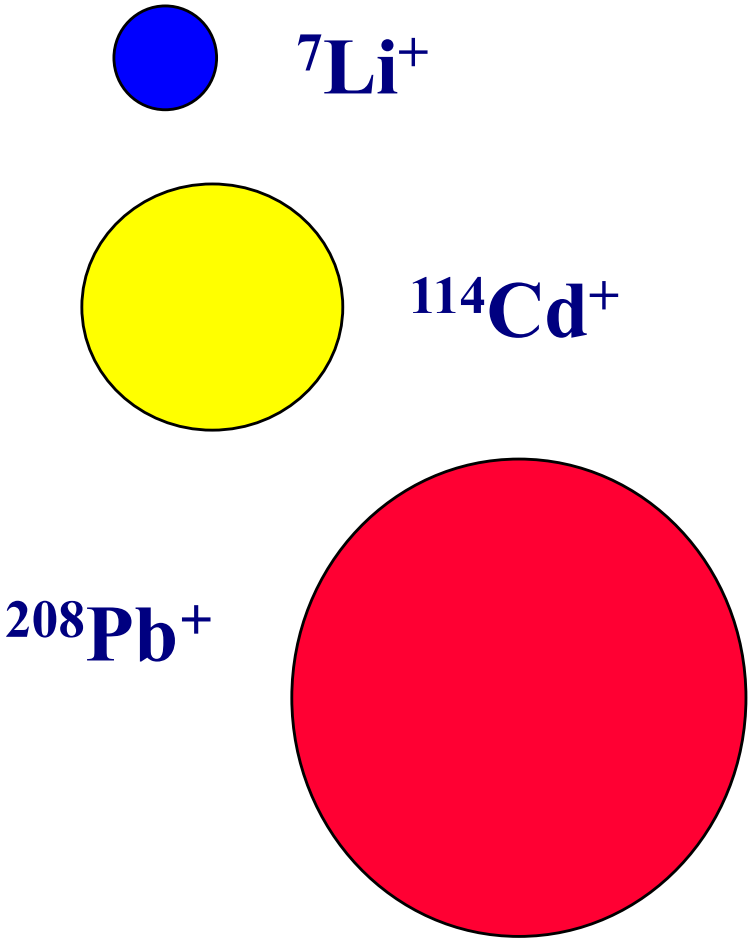

Generic ICP-MS System Hardware

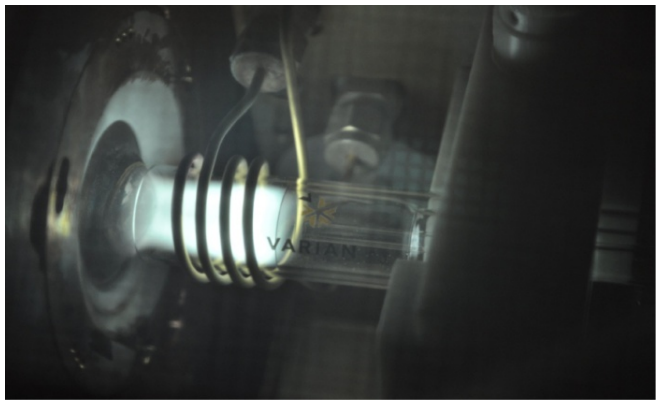

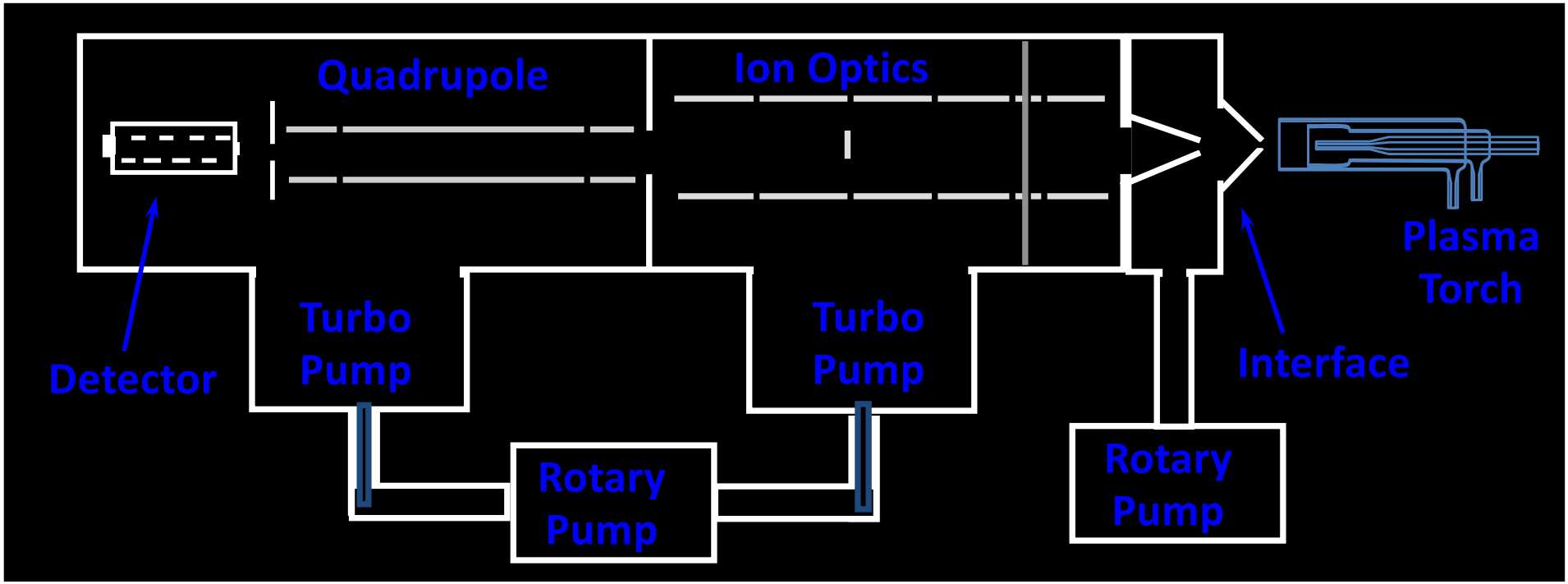

Applications: Forensic Analysis

- **Sample Preparation: Laser Abla**

- Direct Solid Sampling
- Very Little Sample Prep
- Spatially Resolved In Situ Analysi
- Integrated software control

LSX-213 schematic

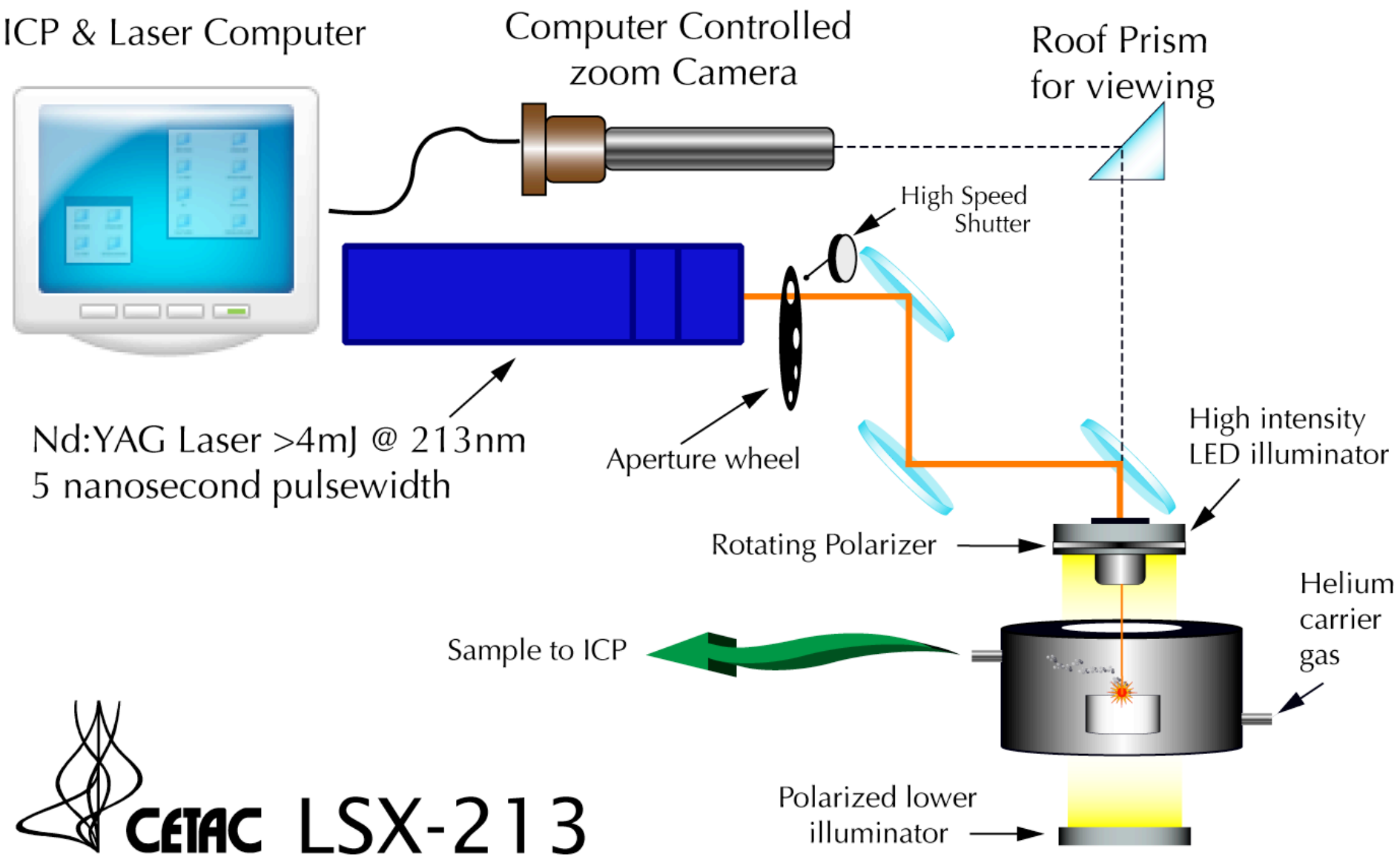

CETAC LSX-213

Ion Optics - Photon Stop Design

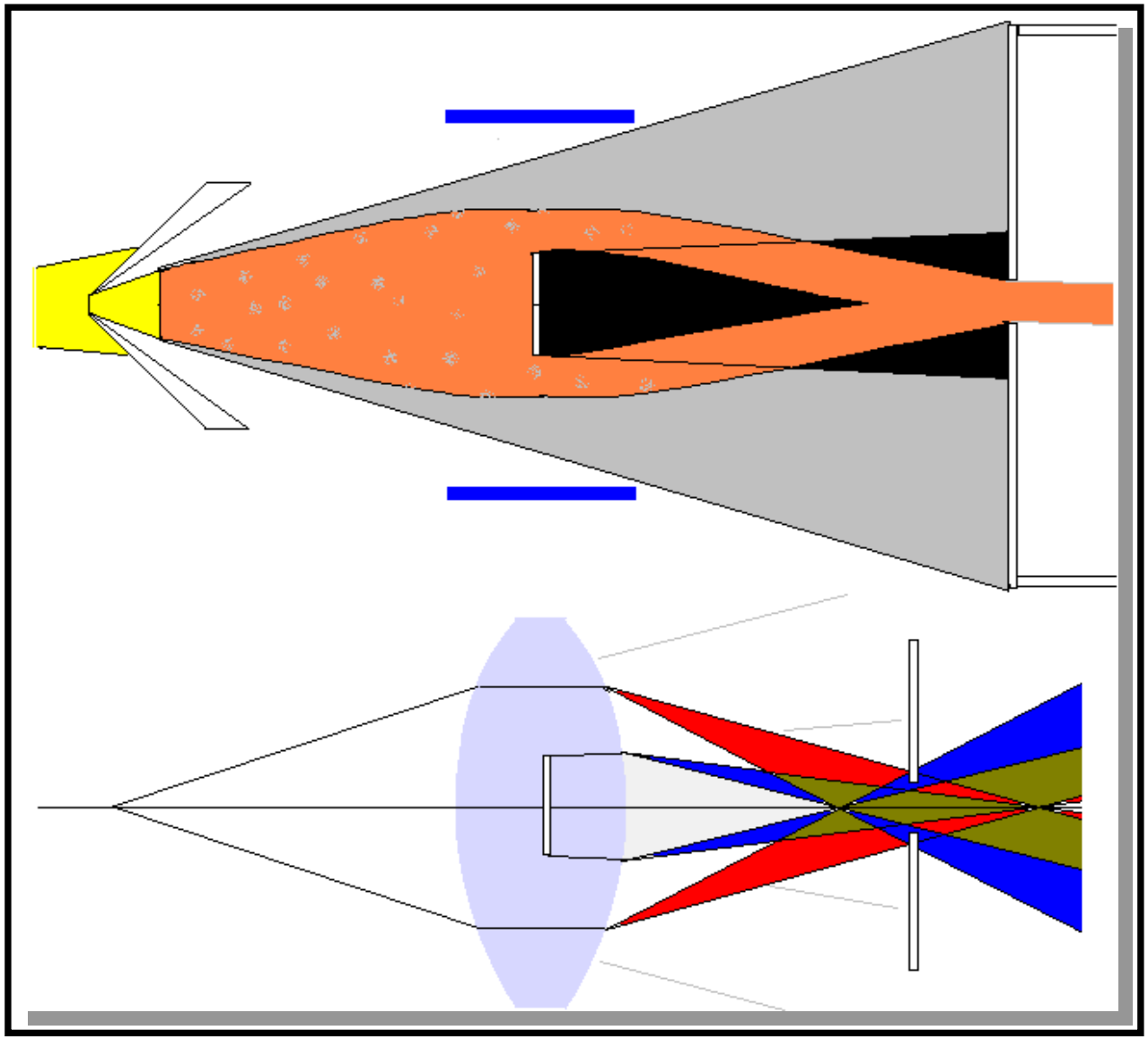

- Ion beam aberrations present
- Optical analogy – note different focal points
- (still used by one competitor)
- **About 10-15% efficient**

4 D Focusing of the Ion Mirror

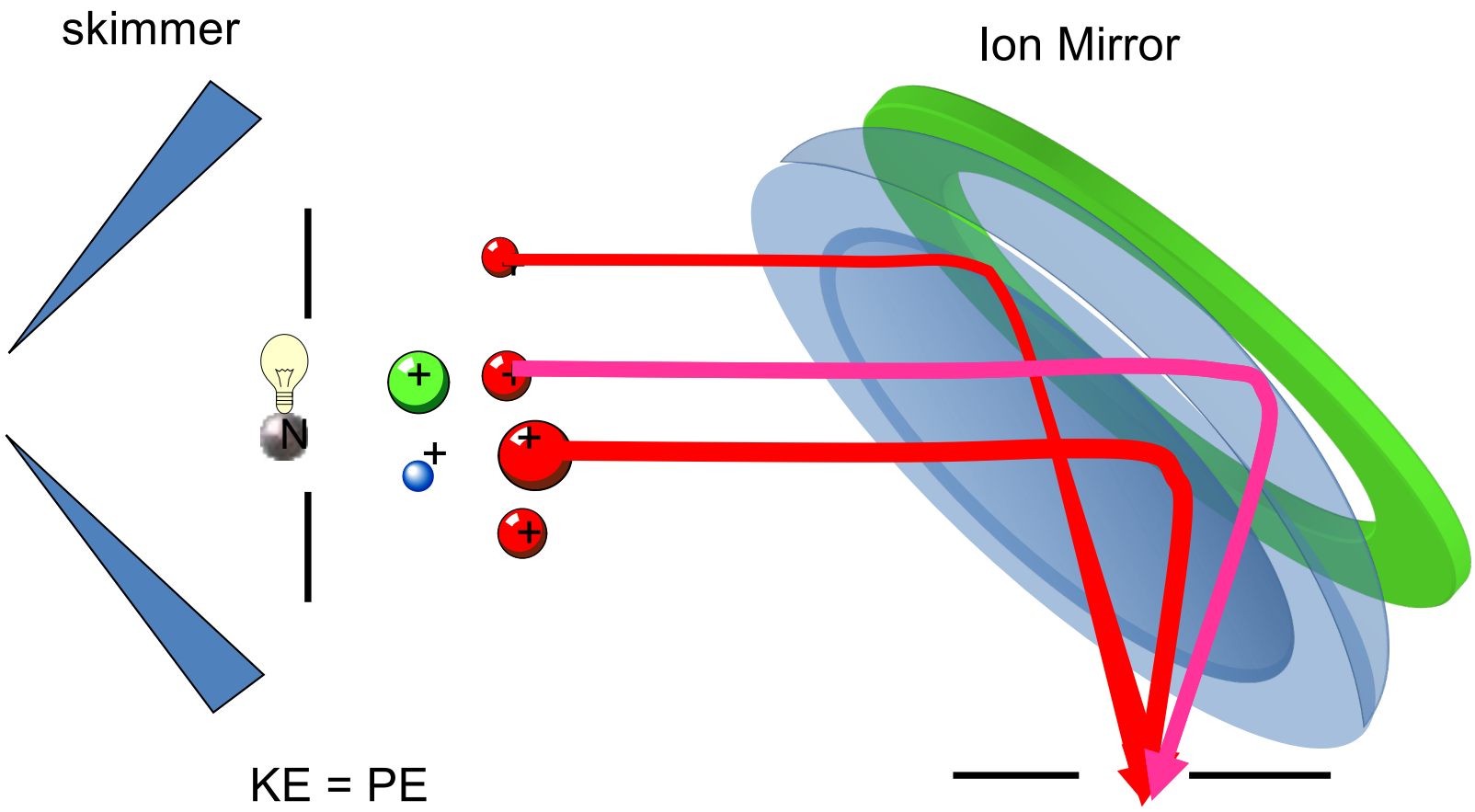

Varians Ion Optics Design – the 90 Degree Ion Mirror

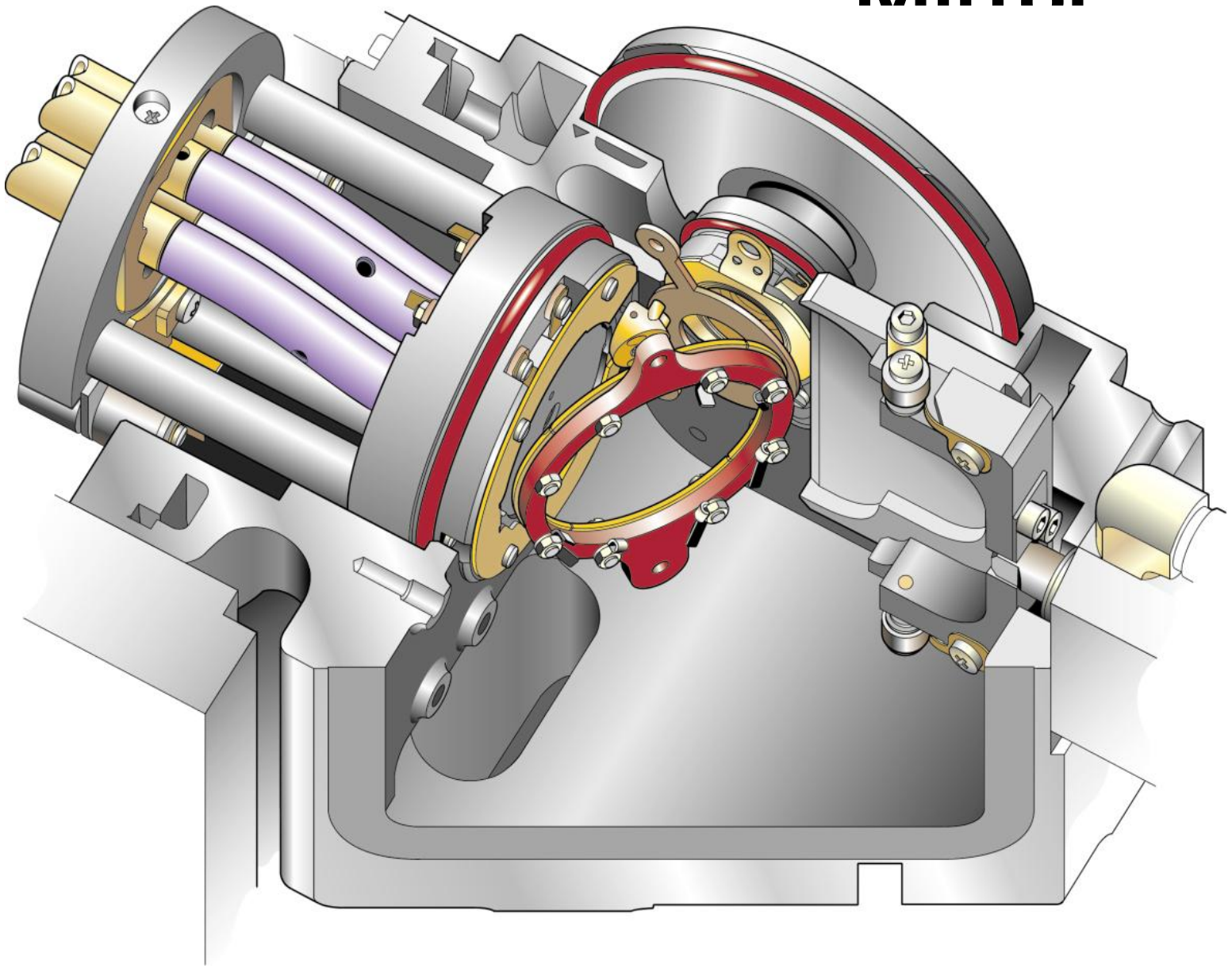

Fractionation

- Fractionation is defined as non-stoichoimetric sampling
- It was originally believed that the laser was causing fractionation at the ablation site
  - This may still happen to some degree with all lasers in metal samples…melting
- Elemental fractionation can occur in three parts of the LA sampling process
  - At the ablation site
  - During transport
  - In the ICP
- Elemental fractionation has been shown to be reduced using lower wavelength lasers as compared to 266 nm system (smaller more easily ionized particles)

Fractionation

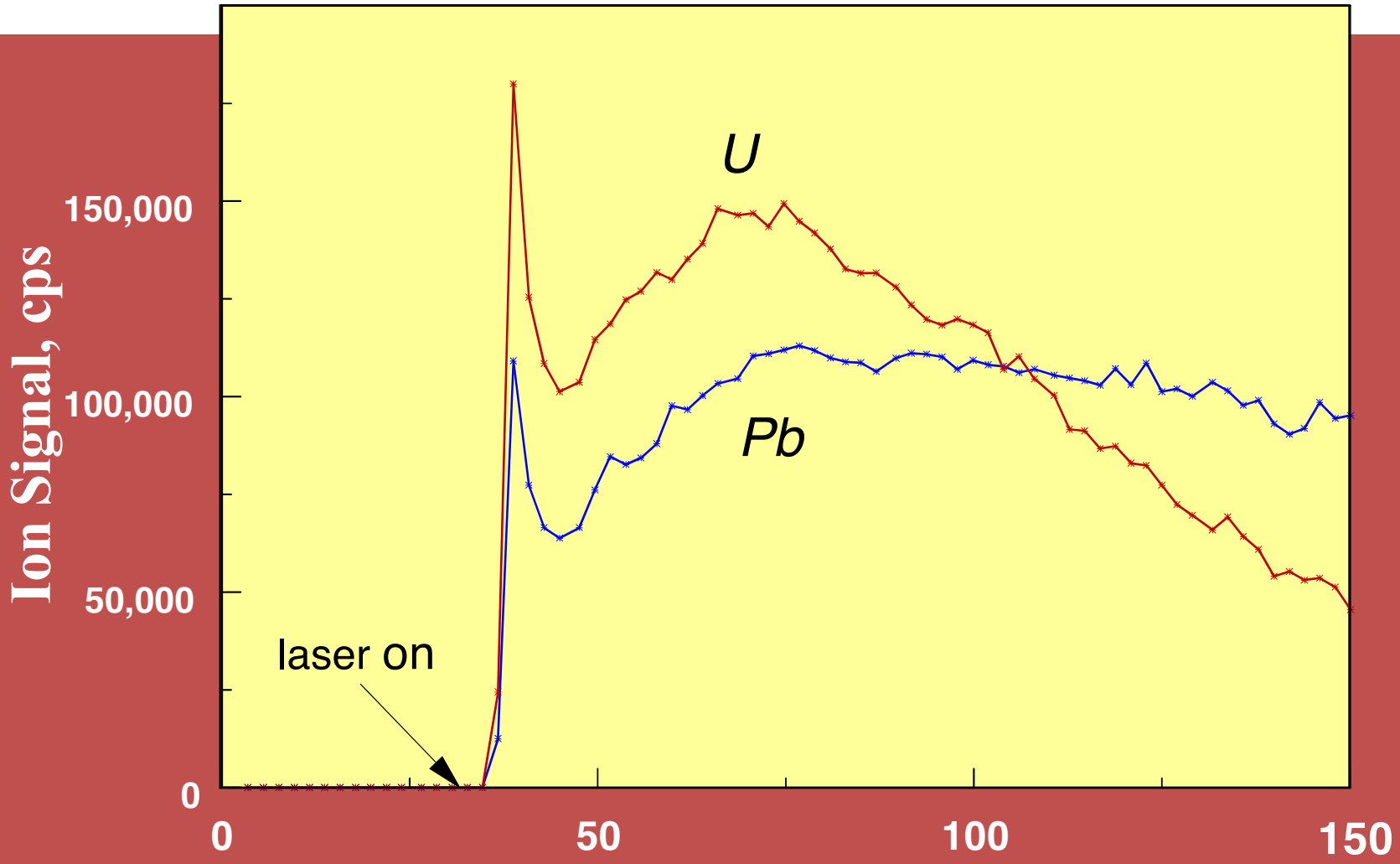

Figure 4- (A) Image of spotted gar liver showing ablations in a macrophage aggregate and normal tissue . ^{202}Hg signal in (B) normal tissue and a (C) macrophage aggregate.

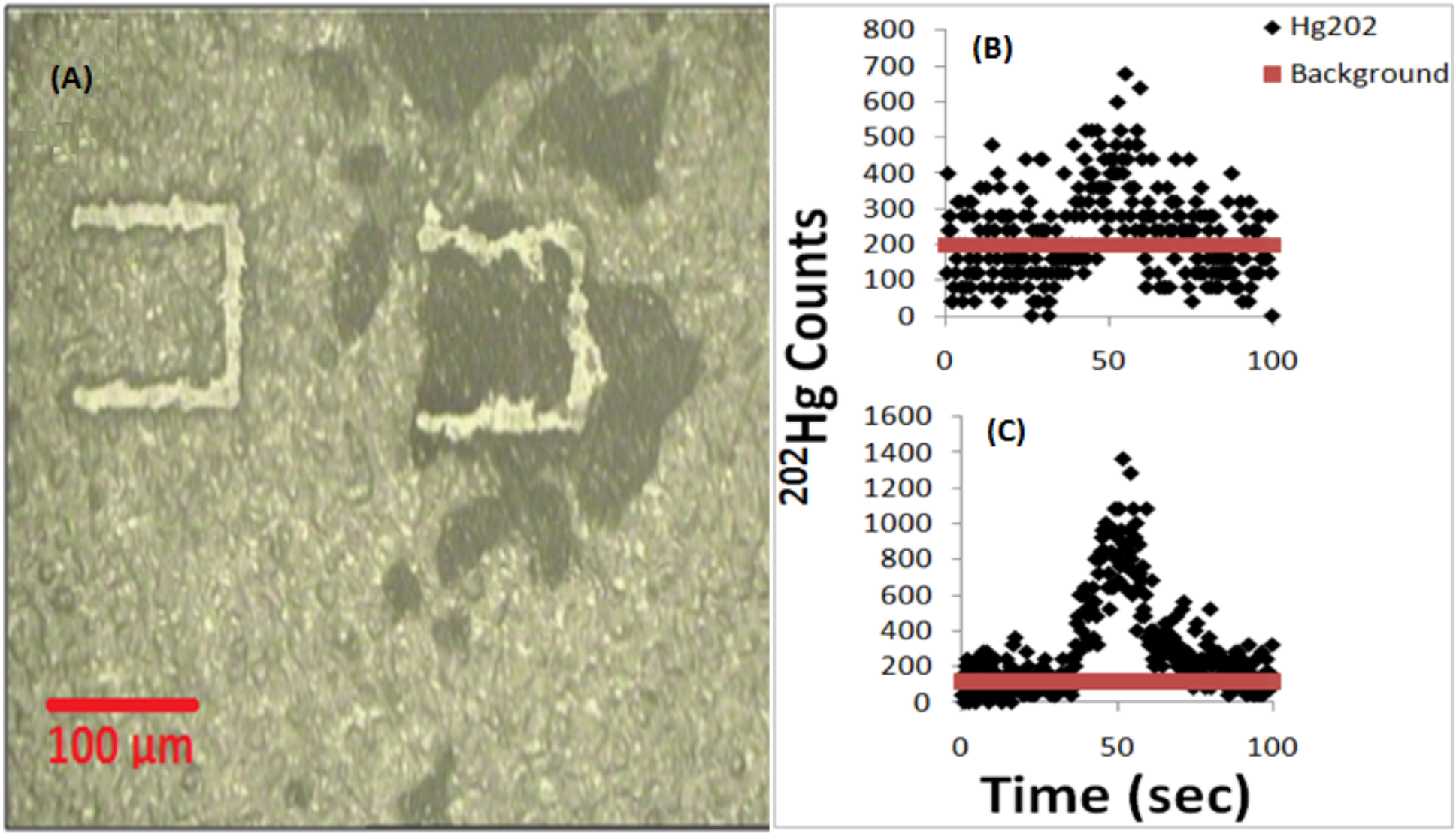

Figure 5- (A) A pre-ablation image of a spotted gar liver section with a superimposed raster pattern . Dark patches are macrophage aggregates. Lighter patches are normal parenchyma. (B) 3D contour image showing the relative distribution of ^{202}Hg after laser ablation of the section shown in (A).

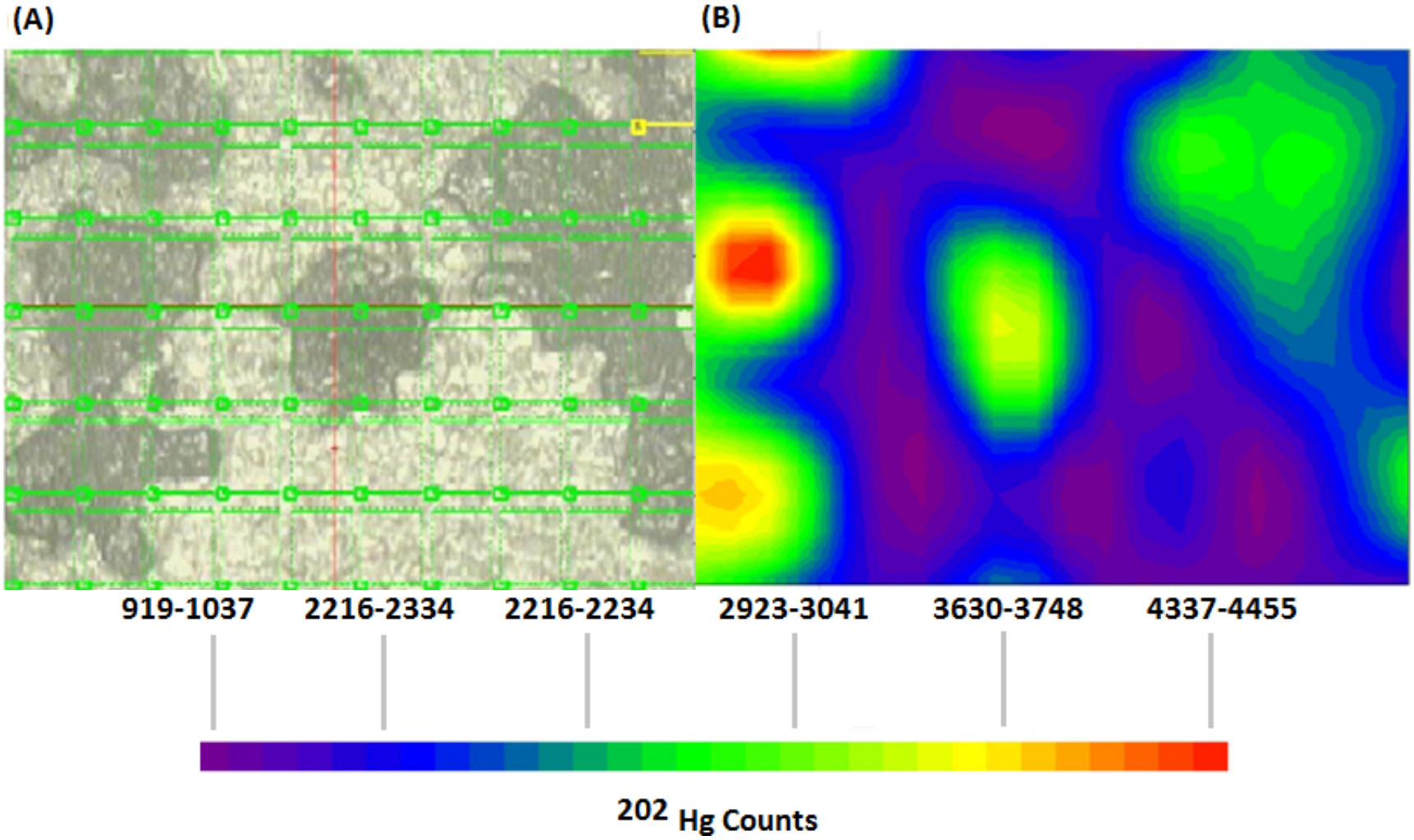

Barst, B.D.; Gevertz, A.K.; Chumchal, M.M.; Smith, J.D.; Rainmater, T.R.; Drevnick, P.E.; Hudelson, Hart, A.; Verbeck, G.F.; Roberts, A.P., "Mercury accumulates in melanomacrophage aggregates in wild fish livers: Evidence of link between mercury exposure and negative effects on the health of wild fish", Science, 2011. *Submitted, In Review*

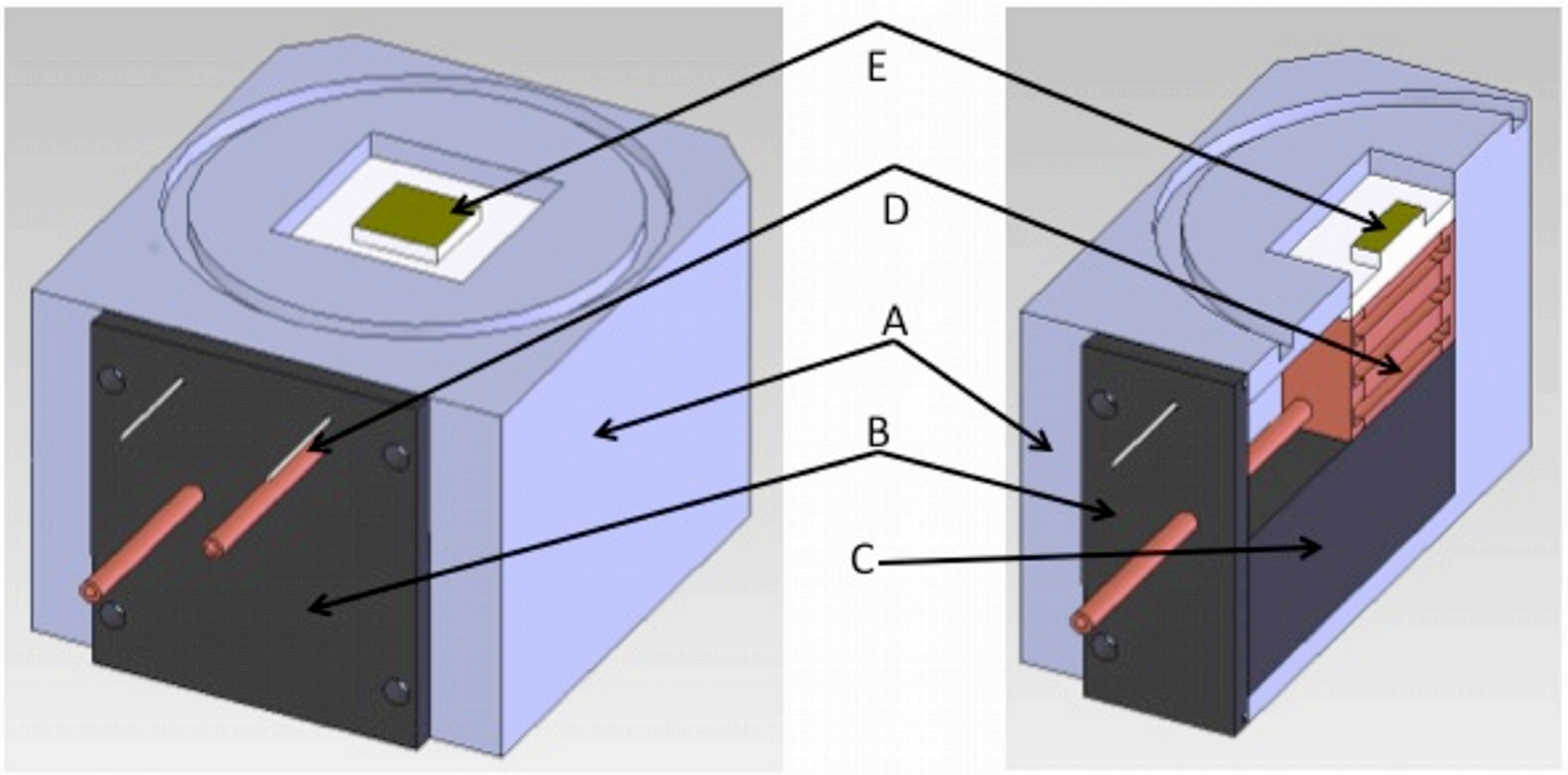

Cold Cell Block

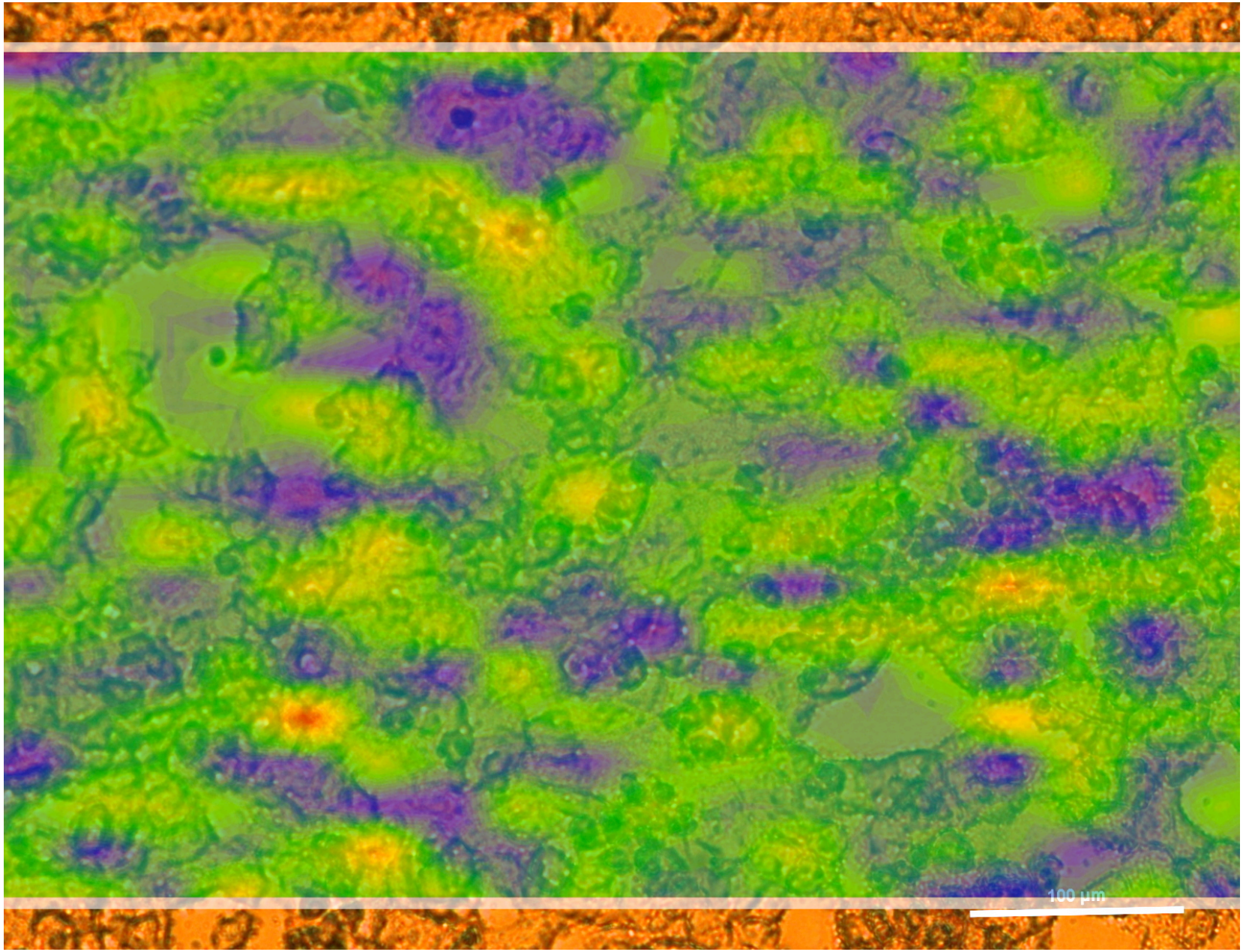

^{102}Ru image mapping in HeLa Cells

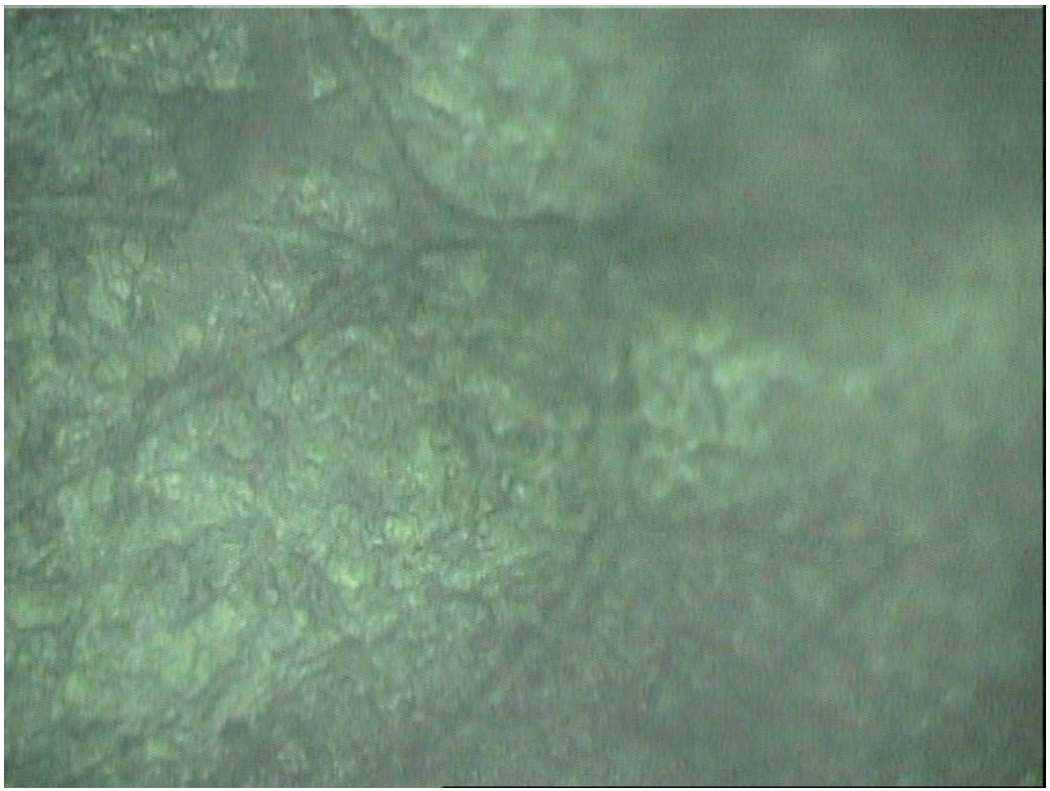

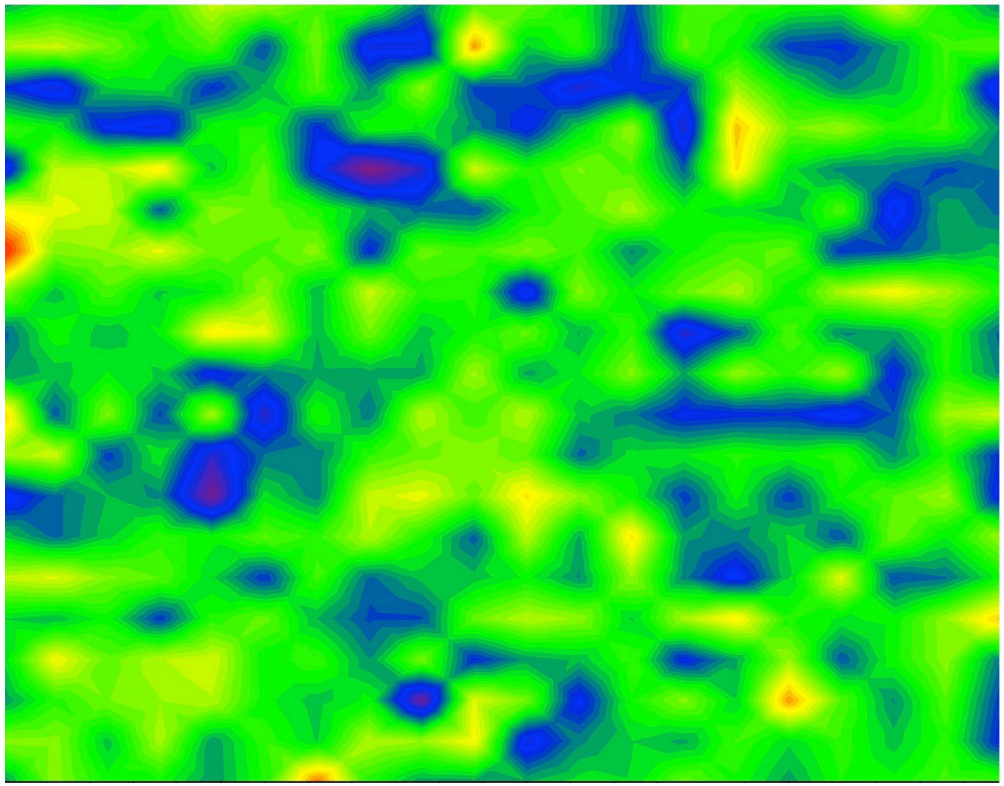

^{39}K Mapping Image of Arabidopsis leaf section
with cold cell LA-ICPMS

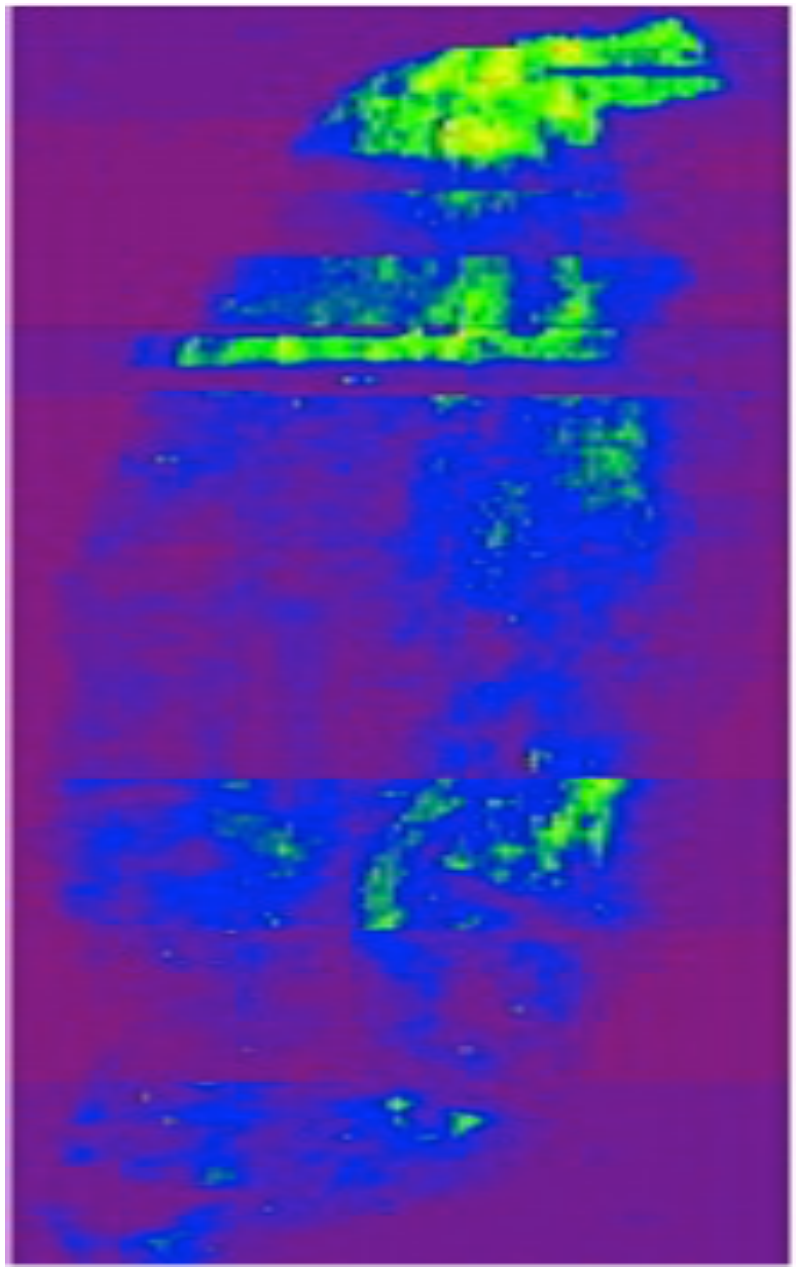

^{23}Na mapping image of Arabidopsis Leaf
cold cell LA-ICPMS

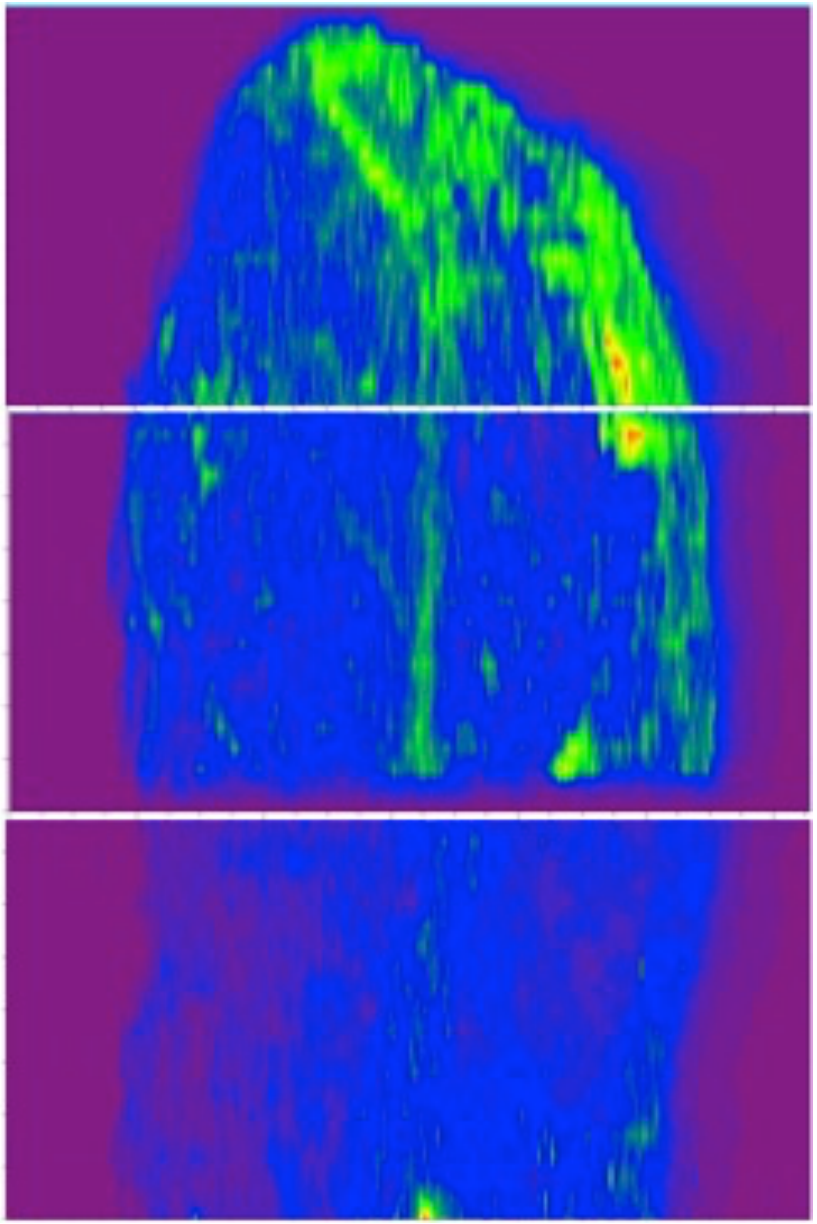

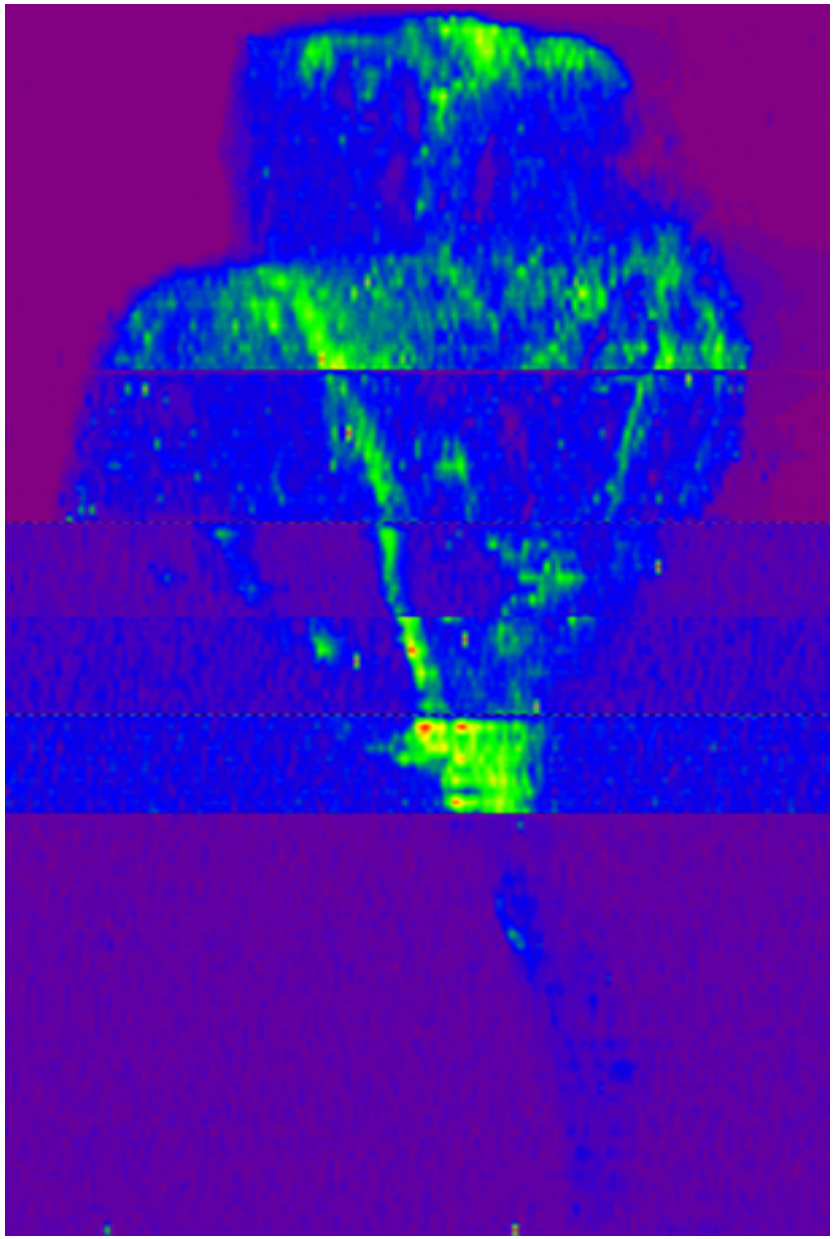

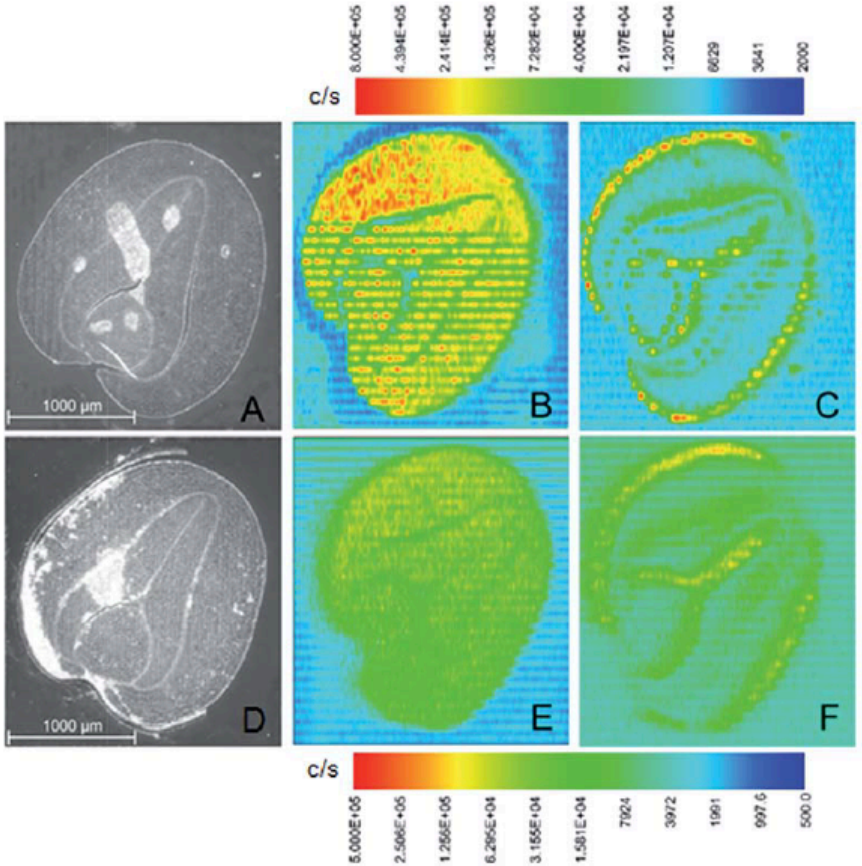

Fig. 3 Top: (A) CCD pre-ablation image of *B. napus* seed section, cooled ablation of ^{31}P (B) and ^{55}Mn (C). Bottom: (D) CCD pre-ablation image of *B. napus* seed section, normal ablation of ^{31}P (E) and ^{55}Mn (F) differences in orientation between the CCD images and elemental images are due to shifts in placement when moving the seed to microscope after ablation. Artefacts in the images are due to the line scan method.

Evaluation of a custom single Peltier-cooled ablation cell for elemental imaging of biological samples in laser ablation-inductively coupled plasma-mass spectrometry (LA-ICP-MS)

J. S. Hamilton,a E. L. Gorishek,a P. M. Mach,a D. Sturtevant,b M. L. Ladage,b N. Suzuki, P. A. Padilla,b R. Mittler,b K. D. Chapmanb and G. F. Verbeck

Evaluation of a custom single Peltier-cooled ablation cell for elemental imaging of biological samples in laser ablation-inductively coupled plasma-mass spectrometry (LA-ICP-MS)

J. S. Hamilton,a E. L. Gorishek,a P. M. Mach,a D. Sturtevant,b M. L. Ladage,b N. Suzuki, P. A. Padilla,b R. Mittler,b K. D. Chapmanb and G. F. Verbeck

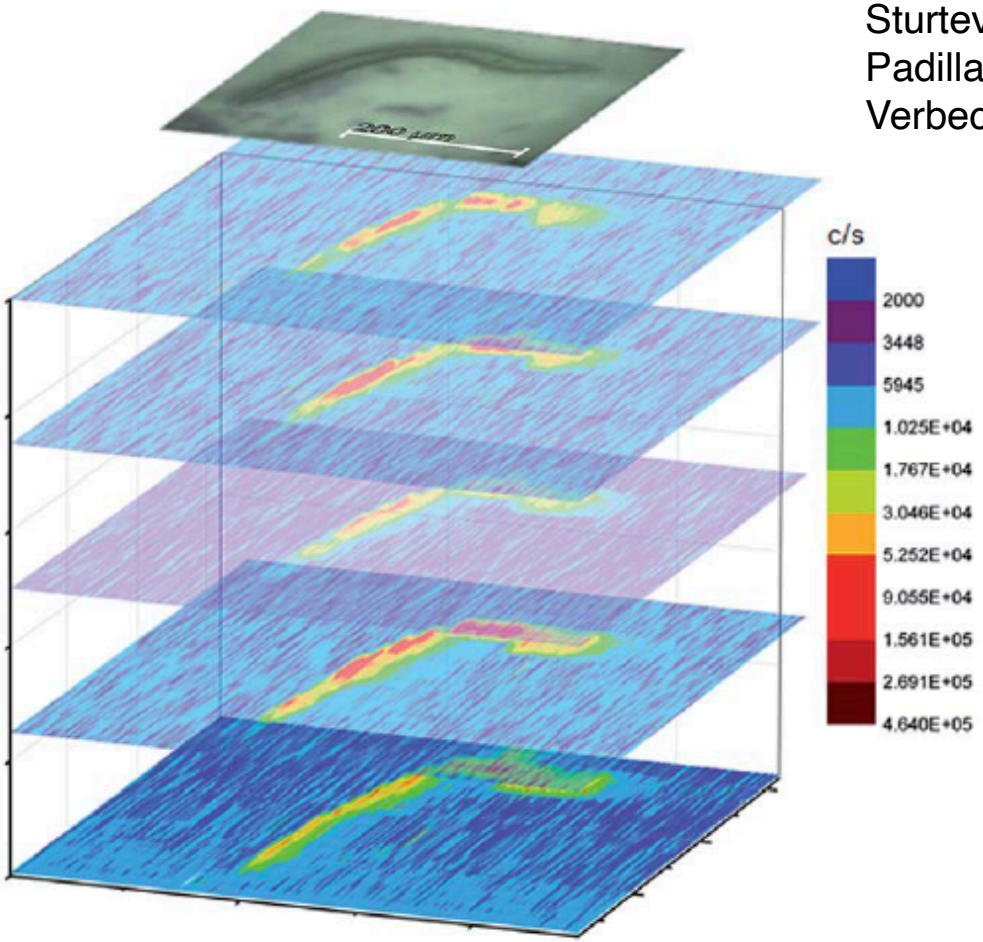

Fig. 4 Stacked 2D measured intensities elemental maps of ^{31}P in a wild type *C. elegans* worm at depth increments of 1.04 μm with an overlaid CCD image of the worm before ablation.